Pharmacological Research 194 (2023) 106850

Contents lists available at ScienceDirect

Pharmacological Research

journal homepage: www.elsevier.com/locate/yphrs

CERS4 predicts positive anti-PD-1 response and promotes immunomodulation through Rhob-mediated suppression of $CD8^+Tim3^+$ exhausted T cells in non-small cell lung cancer

Jian Wang [a,b,1], Run-Ze Li [c,d,1], Wen-Jun Wang [e,1], Hu-Dan Pan [c,d], Chun Xie [f], Lee-Fong Yau [a], Xing-Xia Wang [a], Wei-Li Long [g], Rui-Hong Chen [a], Tu-Liang Liang [c], Lin-Rui Ma [a], Jia-Xin Li [a], Ju-Min Huang [f], Qi-Biao Wu [a], Liang Liu [c,d,*], Jian-Xing He [e,**], Elaine Lai-Han Leung [f,h,***]

[a] *Dr. Neher's Biophysics Laboratory for Innovative Drug Discovery/State Key Laboratory of Quality Research in Chinese Medicine/Macau Institute for Applied Research in Medicine and Health, Macau University of Science and Technology, Macau (SAR), China*
[b] *Department of Medical Oncology, Sichuan Clinical Research Center for Cancer, Sichuan Cancer Hospital & Institute, Sichuan Cancer Center, Affiliated Cancer Hospital of University of Electronic Science and Technology of China, Chengdu, China*
[c] *State Key Laboratory of Traditional Chinese Medicine Syndrome, The Second Affiliated Hospital of Guangzhou University of Chinese Medicine, Guangzhou, Guangdong, China*
[d] *Guangdong-Hong Kong-Macau Joint Lab on Chinese Medicine and Immune Disease Research, Guangzhou, China*
[e] *State Key Laboratory of Respiratory Disease, National Clinical Research Center for Respiratory Disease, Guangzhou Institute of Respiratory Health, The First Affiliated Hospital of Guangzhou Medical University, Guangzhou, China*
[f] *Cancer Center, Faculty of Health Sciences, University of Macau, Macau (SAR), China. MOE Frontiers Science Center for Precision Oncology, University of Macau, Macau (SAR), China. State Key Laboratory of Quality Research in Chinese Medicine, University of Macau, Macau (SAR), China*
[g] *Department of Oncology, Luzhou People's Hospital, Luzhou, Sichuan, China*
[h] *Laboratory of Allergy and Precision Medicine, Chengdu Institute of Respiratory Health, the Third People's Hospital of Chengdu, Affiliated Hospital of Southwest Jiaotong University, Chengdu, China; Department of Pulmonary and Critical Care Medicine, Chengdu Institute of Respiratory Health, Chengdu Third People's Hospital Branch of National Clinical Research Center for Respiratory Disease, Chengdu, China*

ARTICLE INFO

Keywords:
Sphingolipid metabolism
CERS4
NSCLC
ICIs
Rhob
$CD8^+$ $Tim\text{-}3^+$ T cell

ABSTRACT

Non-small cell lung cancer (NSCLC) is one of the main malignant tumors with high mortality and short survival time. Immunotherapy has become the standard treatment for advanced NSCLC, but it has the problems of drug resistance and low response rate. Therefore, obtaining effective biomarkers to predict and enhance immune checkpoint inhibitors (ICIs) efficacy in NSCLC is important. Sphingolipid metabolism is recently found to be closely involved in tumor immunotherapy. CERS4, an important sphingolipid metabolizing enzyme, is positively correlated with the efficacy of anti-PD-1 therapy for NSCLC. Upregulation of CERS4 expression could improve the efficacy of anti-PD-1 therapy for NSCLC. High expression of CERS4 could downregulate the expression of Rhob in tumor. Significantly, the ratio of $CD4^+/CD8^+$ T cell increased and the ratio of $Tim\text{-}3^+/CD8^+$ T cell decreased in spleen and peripheral blood cells. When Rhob was knocked out, the efficacy of PD-1 mAb treatment

Abbreviations: α-GalCer, α-Galactose ceramide; ATCC, American Type Culture Collection; BP, biological process; CC, cellular component; CerP/C1P, ceramide-1-phosphate; CERS, ceramide synthase; DMEM, Dulbecco's Modified Eagle Medium; FBS, fetal bovine serum; FDA, Food and Drug Administration; FoxP3, forkhead box protein P3; ICIs, immune checkpoint inhibitors; IHC, immunohistochemistry; iNKT, invariant natural killer T; IOD, integrated optional density; LC-MS, liquid chromatography-mass spectrometry; LLC, lewis lung carcinoma; mAb, monoclonal antibody; MF, molecular function; MMR, mismatch repair; MSI, microsatellite instability; NSCLC, non-small cell lung cancer; nSMase2, neutral SMase 2; PCA, principal component analysis; PFS, progression-free survival; PS, penicillin-streptomycin; QC, quality control; RECIST, response evaluation criteria in solid tumors; SK1, sphingosine kinase 1; SM, sphingomyelin; TILs, tumor-infiltrating lymphocytes; TMB, tumor mutation burden.

* Corresponding author at: State Key Laboratory of Traditional Chinese Medicine Syndrome, The Second Affiliated Hospital of Guangzhou University of Chinese Medicine, Guangzhou, Guangdong, China.
** Corresponding author.
*** Corresponding author at: Cancer Center, Faculty of Health Sciences, University of Macau, Macau (SAR), China. MOE Frontiers Science Center for Precision Oncology, University of Macau, Macau (SAR), China. State Key Laboratory of Quality Research in Chinese Medicine, University of Macau, Macau (SAR), China.
E-mail addresses: lliu@gucm.edu.cn (L. Liu), drjianxing.he@gmail.com (J.-X. He), lhleung@um.edu.mo (E.L.-H. Leung).
[1] These authors contribute equally.

https://doi.org/10.1016/j.phrs.2023.106850
Received 25 May 2023; Received in revised form 8 July 2023; Accepted 10 July 2023
Available online 13 July 2023

increased, and the frequency of Tim-3$^+$ CD8$^+$ T cell decreased. This finding further confirmed the role of sphingolipid metabolites in regulating the immunotherapeutic function of NSCLC. These metabolites may improve the efficacy of PD-1 mAb in NSCLC by regulating the CERS4/Rhob/Tim-3 axis. Overall, this study provided a potential and effective target for predicting and improving the efficacy of ICIs for NSCLC. It also provided a new perspective for the study on the mechanisms of ICIs resistance for NSCLC.

1. Introduction

Lung cancer is the most common malignant tumor in the world [1]. Non-small cell lung cancer (NSCLC) represents for more than 80% of lung cancer, with numerous patients clinically diagnosed as locally advanced or distant metastases with poor prognosis [2–4]. ICIs therapy has become the main treatment for NSCLC, especially in advanced stage [5–8]. However, it has the problems of drug resistance and low response rate. Finding effective indicators to predict and improve the response rate of ICIs for NSCLC has become an important research direction.

At present, some biomarkers have been reported to predict and regulate the efficacy of ICIs for NSCLC. PD-L1 expression is a consensus biomarker [9,10]. However, even though the PD-L1 tumor proportion score of patients with NSCLC is more than 50%, the 5-year overall survival was only 29.6% for newly treated and 25.0% for previously treated patients [10]. Clinical studies have shown that ICIs in patients with NSCLC with a high tumor mutation burden (TMB) leads to enhanced outcomes, and the 1-year progression-free survival rate is 42.6% [11]. In another clinical phase II study, high TMB status has also shown to confer a robust antitumor ICIs response in solid tumors [12]. Some other biomarkers include tumor-infiltrating lymphocytes (TILs) [13], microsatellite instability /mismatch repair [14,15], and driver gene mutation [16,17]. However, none of these measures has worked well. Therefore, effective biomarkers to predict and regulate the efficacy of ICIs for NSCLC are urgently needed.

According to recent reports, sphingolipid metabolism is closely related to cancer immunotherapy[18]. Sphingolipid metabolites could induce the excretion of immune cells from lymphoid organs into the blood and regulate the antitumor function of various immune cell types [19]. α-Galactose ceramide (α-GalCer) has the function of activating invariant natural killer T (iNKT) lymphocytes. α-GalCer combined with PD-1 blocker prevented iNKT cell loss and tilted CD4 + cells towards Th1 [20]. The fusion of α-GalCer with CD1D-SCFV protein led to the sustained activation of iNKT cells and superior tumor control [21]. Moreover, SPHK1-produced S1P was directly linked to the activity of the lipid transcription factor peroxisome proliferator-activated receptor γ, which subsequently regulates lipolysis in T cells [22]. In mouse models of melanoma, breast cancer, and colon cancer, knockdown of sphingosine kinase 1 (SK1) significantly enhanced the efficacy of ICIs [23]. Another study reported that neutral SMase 2 (nSMase2) has the function of regulating ICIs efficacy. In mouse models of melanoma and breast cancer, overexpression of wild-type nSMase2 increased anti-PD-1 efficacy, which is associated with increased levels of transcripts encoding IFNγ and CXCL9 [24]. As such, regulating the sphingolipid metabolism pathway may be an effective method to improve the efficacy of immunotherapy. Thus, targeting the regulators of sphingolipid signaling pathways to improve the efficacy of cancer immunotherapy is a broad research prospect.

In addition to basic research, sphingolipid metabolites show broad promise in clinical applications. Some clinical studies have been carried out on sphingolipid metabolism in antitumor and immune regulation [25–27], and positive effects have been obtained. Takahide et al. found that α-galactosylceramide pulsed antigen presenting cells showed good efficacy in patients with advanced or recurrent NSCLC[26]. By combining ceramide with other fatty lipids, researchers at Penn State University have developed a new compound that significantly improves its stability in the body, targeting cancer cells for destruction while not harming healthy cells. The compound has been approved by the U.S. Food and Drug Administration for clinical trials (https://www.psu.edu/news/research/story/investigational-cancer-compound-receives-fda-approval-begin-human-trial S). Phase I studies of C6 ceramide nanoliposomes in the treatment of advanced solid tumors have also been conducted (NCT02834611). Together, sphingolipid metabolism has shown initial value in antitumor clinical application.

Despite the tremendous research ongoing in this field, the correlation between sphingolipid metabolism and immunotherapy in NSCLC remains to be fully understood. In this study, sphingolipid analysis was applied on NSCLC clinical samples. A promising target that may modulate the efficacy of ICIs for NSCLC was identified. The role of this target was further validated through cellular and animal experiments, and the mechanism was further explored by transcriptomic analysis to identify the role of CERS4 in enhancing efficacy of ICIs through modulating Rhob. Studying this new target may provide new strategies to improve the immunotherapeutic efficacy of NSCLC in clinical practice.

2. Methods and materials

2.1. Sphingolipid metabolism analysis methods

All blood samples were collected by the staff of the First Affiliated Hospital of Guangzhou Medical University. Blood samples (5 mL) were centrifuged at 3000 rpm for 15 min within 30 min after the blood sample was drawn. The separated serum was stored at − 80 °C. Sphingolipid components were extracted using an established method [28]. Each sample was prepared in duplicate and detected by liquid chromatography–mass spectrometry (LC–MS). Quality control samples were pooled with equal amounts of samples from different groups for sphingolipid identification. An in-house sphingolipid database was created in the lab for data analysis. This database is based on the Agilent MassHunter personal compound database and the information from the LIPID MAPS lipidomics gateway. The identification of sphingolipids was on the basis of high-resolution MS and MS/MS data. Raw data for quantitative analysis were processed with Agilent MassHunter Quantitative Analysis B.06.00 software. Multivariate statistical analyses were performed with SIMCA-P + 14.0 software (Umetrics, Umea, Sweden). Principal component analysis was used to visualize the general clustering between different groups.

2.2. Cell culture

Human normal lung epithelial cells (BEAS-2B and Nuli-1), human lung cancer cells (A549, H358, H2122, H1975, HCC827, PC-9, H1650, H23, H1299, and H460), and mouse lung cancer cells [Lewis lung carcinoma (LLC)] were purchased from American Type Culture Collection (ATCC). The A549, H358, H2122, H1975, HCC827, PC-9, H1650, H23, H1299, and H460 cells were cultured in RPMI-1640 medium containing 10% fetal bovine serum (FBS) and 1% penicillin–streptomycin (PS). The LLC cells were cultured with Dulbecco's modified Eagle medium supplemented with 10% FBS and 1% PS. The BEAS-2B cells were grown in a BEGM medium. The Nuli-1 cells were grown in an airway epithelial cell basal medium (ATCC PCS300030). All cells were maintained at 37 °C at a 5% CO_2 incubator.

2.3. Reagents and antibodies

The antibodies used were anti-α-tubulin (2125, CST, Danvers, MA,

USA), anti-β-actin (4970, CST), anti-mouse CERS4 (PA5–49881, Thermo Fisher Scientific, Carlsbad, CA, USA), anti-human CERS4 (PA5–50695, Thermo Fisher Scientific), anti-rabbit Rhob (63876, CST), PerCP/Cyanine5.5 anti-mouse CD3 (100218, Biolegend, San Diego, CA, USA), FITC anti-mouse CD4 (100510, Biolegend), PE/Cyanine7 anti-mouse CD8a (100722, Biolegend), and PE anti-mouse CD366 (Tim-3; 119704, Biolegend). All Western blot antibodies were used at 1:1000 dilution, and IHC antibodies were used at 1:100 dilution.

2.4. Protein extraction and Western blot

Cells were harvested and lysed with RIPA buffer (P0013B, Beyotime, Shanghai, China), which contained 1 mM PMSF (ST506, Beyotime). Protein concentrations were quantitatively measured by BCA Protein Assay Kit (P0012S, Beyotime), and the appropriate amount of protein sample was loaded on SDS polyacrylamide gels. After electrophoresis, the samples were transferred to a PVDF membrane. Then, the membrane was blocked, incubated with primary and secondary antibodies, and developed with enhanced chemiluminescence.

2.5. qPCR and PCR

Total RNA was prepared by TRIzol (Invitrogen, CA, USA) and reverse transcribed to cDNA by TransScript All-in-One First-Strand cDNA Synthesis SuperMix for qPCR (One-Step gDNA Removal; TransGen Biotech, AT341–03). PerfectStart Green qPCR SuperMix (+Dye II; TransGen Biotech, AQ602–23) was used to analyze the mRNA expression. The total RNA (1 μg) was reverse transcribed using the miRNA 1st Strand cDNA Synthesis Kit (by stem-loop, Vazyme, MR101). MiRNA Universal SYBR qPCR Master Mix (Vazyme, MQ101) was used to analyze the miRNA expression. The sequences of all qPCR primers used in this research are listed in Extended Data Table 1. The 2-ΔΔCt method was used to analyze the qRT-PCR results.

2.6. Lentivirus plasmid construction and transfection experiment

CERS4 overexpression lentivirus plasmid was constructed by Sangon Biotech (Shanghai, China). Human lung cancer cell lines A549, H1299, and H1975 were transfected using polybrene. Mouse lung cancer cell line LLC were transfected using polybrene. The medium was changed after 24 h, and the cells were cultured for another 48 h. The cells were then selected with puromycin (2 μg/mL) for 14 days for further experiments.

2.7. MTT assay

The proliferation rate of cells was examined by MTT assay. The percentages of cell viability of the A549, H1299, H1975, and transfected CERS4 lentivirus plasmid cell lines were calculated as the percentage change in the absorbance of treated cells divided by the absorbance of untreated cells.

Table 1
Clinical characteristics of 12 NSCLC patients with treatment of PD-1 mAb.

characteristics	PD-1 mAb	
	Responder	Non-responder
Age (years)	6	6
≤ 65	4	5
> 65	2	1
gender	6	6
male	4	3
female	2	3
pathology	6	6
squamous carcinoma	3	4
adenocarcinoma	3	2
TNM stage	IV	IV

2.8. Colony formation assay

Colony formation assay was performed to evaluate the effect of CERS4 overexpression on the growth activity of NSCLC cell lines (A549, H1299, and H1975). The cells (1000) were plated into six-well plates and allowed to adhere overnight or 24 h. They were then cultured for 14 days to form colonies. The medium was changed every 3 days.

2.9. Animal experiments

All animal experiments were approved by the Use and Care of Animals Committee at Macau University of Science and Technology. C57BL/6 J mice aged 8–10 weeks were reared in independently vented cages at the animal facility of the State Key Laboratory of Quality Research in Chinese Medicine, Macau University of Science and Technology. Approximately 5×10^5 LLC cells and LLC^{CERS4+} cells were subcutaneously inoculated into the right flanks of the mice. After 3 days of tumor grafting, PBS and αPD-1 monoclonal antibody (mAb; 250 μg/mouse, clone: RMP 1–14, Bio X Cell) were intraperitoneally injected. A total of 40 mice from different litters were equally divided into four groups: LLC group (treated with PBS), LLC PD-1 group (treated with αPD-1 mAb), LLC^{CERS4+} group (treated with PBS), and LLC^{CERS4+} PD-1 group (treated with αPD-1 mAb). PBS or αPD-1 mAb was injected six times at 3-day intervals. The tumor volumes and body weights were measured every 3 days. The survival curve was calculated by GraphPad Prism 7.0 software.

2.10. RNA sequencing

Total RNA was prepared by TRIzol (Invitrogen, CA, USA). Illumina HiSeq 4000 sequencing was performed by LC-BIO Technologies (Hangzhou, China) Co., Ltd. The OmicStudio tool is located at https://www.omicstudio.cn/tool, and it was used for bioinformatics analysis.

2.11. Flow cytometry

At the endpoint of the animal experiment, the blood and spleen were harvested for flow cytometric analysis. For FACS analysis, single-cell suspensions were stained with the following antibodies: anti-mouse CD3, CD4, CD8a, and CD366 (Tim-3). The analysis was performed using a FACSArial III flow cytometer (BD, USA). Data were analyzed using FlowJo software (version 10.4, FlowJo, USA).

2.12. Immunohistochemistry (IHC)

Tissues were fixed, paraffin embedded, and dewatered. The paraffin blocks were cut into sections. The paraffin-embedded sections were dewaxed in xylene and hydrated with a graded ethanol solution. All samples were stained with an IHC kit (K8002; Dako, Glostrup, Denmark). The primary antibodies used were anti-CERS4 (1:100). Each section was counterstained with hematoxylin and sealed with resin. Slides were scanned and observed under a Leica optical microscope (Leica Biosystems Imaging, USA).

2.13. Constructed Rhob knockout LLC cell line for animal experiment

Rhob knockout was generated by Cyagen (Suzhou, China). The LLC cell line was tested for clearance from bacteria, mold, mycoplasma, and other contaminants. Clonal efficiency was observed to determine cell proliferation. The region containing the mutation was sequenced to confirm the genotype. The model was created by CRISPR/Cas9-mediated genome engineering. Single clones were isolated and enriched for screening. Colonies was genotyped by PCR and sequencing to validate the successful knockout. Positive clones were cryopreserved. The animal experiment was same as the above (LLC^{CERS4+} cell line was changed to LLC^{Rhob-} cell line).

2.14. Statistical analysis

Statistical analyses and graphing were performed using GraphPad Prism 9.0 software. The data in this study were represented as mean ± SD unless otherwise noted. We used an unpaired t-test to compare the averages between two groups. We used ANOVA to compare the averages between multiple groups. We used Kaplan-Meier method to draw survival curves. We used Log-Rank test for comparisons between groups. $P < 0.05$ was regarded as statistically significant.

3. Results

3.1. High level of ceramides and low level of sphingosines are associated with good efficacy of anti-PD1 therapy

For profiling of the sphingolipid metabolites, LC–MS was applied to examine the serum from 12 patients with NSCLC who received anti-PD-1 therapy. All patients agreed to participate in the study and signed informed consent forms. Among them, six were responders and the other six were non-responders. The clinical characteristics of the patients are listed in Table 1. The MRM chromatograms of all sphingolipids in human serum are shown in Extended Data Fig. 1A. In the PLS-DA plot, the sphingolipid biomarkers of responders and non-responders were clearly separated. The PLS-DA score plot showed the discrimination between good and bad effect [R2X(cum): 0.827, R2Y(cum): 0.960, Q2 (cum): 0.770; Fig. 1A]. Analysis of ceramide revealed that patients with better treatment response showed higher ceramide. Ceramide (d18:0/22:0), ceramide (d18:2/22:0), ceramide (d18:1/23:0), ceramide (d18:0/24:0), and ceramide (d18:2/24:0) were significantly higher in the responder group than in the non-responder group (Fig. 1B–1 F). Analysis of sphingomyelin (SM) revealed that patients with better treatment response showed higher SM. SM (d18:2/22:0) was significantly increased in the response group (Fig. 1G). The others, included SM (d18:1/13:0), SM (d18:1/14:0), SM (d18:1/14:1), SM (d18:1/16:0), SM (d18:1/17:1), SM (d17:1/22:0), SM (d17:0/24:0), SM (d18:1/23:0), SM (d18:2/23:0), SM (d18:2/24:0), and SM (d18:2/25:0) in the responder group were significantly higher than those in the non-responder group (Extended Data Fig. 1B and C). In summary, ceramide (d18:0/22:0) and ceramide (d18:2/22:0) were significantly higher in the responder group, and the SM (d18:2/22:0) was also significantly higher in the responder group. When analyzed in conjunction with the sphingolipid metabolic pathway map (Fig. 1H), the high expression of the metabolic enzyme ceramide synthase (CERS) was possibly responsible for this result. CERS is well known to possess six subtypes, and exactly which of them play an important role in modulating efficacy of ICIs must be defined. Among the six CERS isoforms, CERS4 has high selectivity for long and very long (C18:0-C22:0) chains [29,30]. This is consistent with the results of the sphingolipid analysis where ceramide (d18:0/22:0), ceramide (d18:2/22:0), and SM (d18:2/22:0) were all elevated. These data suggested that CERS4 may be an important target for predicting and modulating the efficacy of ICIs in NSCLC.

3.2. CERS4 was selected from six subtypes and closely related to NSCLC prognosis and the efficacy of ICIs

To further validate whether CERS4 is a target for predicting and modulating the efficacy of ICIs in NSCLC. The data from TCGA was used to analyze the correlation of survival with these six subtypes to define the useful response predictive subtype. Given the few data on the direct correlation between CERS and ICIs response in NSCLC, ICIs responders are often predicted to have better outcomes and longer survival time. Therefore, the correlation between the six subtypes of CERS and NSCLC prognosis was analyzed. The results showed that CERS1, CERS2, CERS3, CERS5, and CERS6 and the survival of patients with NSCLC were not clearly correlated (Extended Data Fig. 2A-2E). Meanwhile, CERS4 was positively correlated with the survival of patients with NSCLC, and the patients with high CERS4 expression demonstrated longer survival ($P = 0.00057$, Fig. 2A and B). Similar results were obtained in UCSC data bank, that is, CERS4 expression was positively correlated with the prognosis of patients with NSCLC, and those with high CERS4 expression in tumor tissue had longer survival time ($P = 0.001516$,Fig. 2C). Therefore, CERS4 is likely the subtype closely related to NSCLC prognosis.

Tumor tissue sections from 14 patients with NSCLC receiving PD-1 mAb treatment from Luzhou People's Hospital were collected to further predict and validate the correlation between CERS4 expression levels and efficacy of ICIs in patients with NSCLC. All patients agreed to participate in the study and signed informed consent forms. Among them, seven patients were responders and the other seven were non-responders (the clinical characteristics of patients are listed in Table 2). Patient clinical response was determined on the basis of immune Response Evaluation Criteria in Solid Tumors consistent with published trials in lung cancer [31,32], as shown by the CT scan in Extended Data Fig. 3A and B. IHC was used to detect the CERS4 expression levels in tumor tissues. The results showed that the CERS4 expression levels were higher in the responders than in the non-responders (Fig. 2E). The integrated optional density (IOD) value of IHC was significantly higher in the responder group (Fig. 2D). This result was consistent with the prediction results of the present study, further indicating that CERS4 is a potential predictive marker for the efficacy of ICIs in patients with NSCLC.

3.3. Overexpression of CERS4 in NSCLC cells did not affect growth and viability

Cellular experiments were performed, and 10 human-derived lung cancer cell lines and two normal lung epithelial cells were selected for examination to further verify whether CERS4 is a ICIs therapy predictive and regulatory gene for NSCLC. First, the CERS4 expression levels of the cell lines were detected by PCR. The results showed that the CERS4 expression in normal lung epithelial cell (BEAS2B) was significantly higher than that in human-derived lung cancer cell lines in qPCR (Fig. 3A). Consistent results were obtained by conventional PCR and Western blot (Extended Data Fig. 4A and B). Therefore, CERS4 may be a prognostically beneficial gene, and similar conclusions were reached in the previous bioinformatics analysis and clinical sample validation.

Then, CERS4 overexpressing lung cancer cell lines were constructed by transfection with CERS4 lentiviral plasmids for further functional validation. Three human-derived NSCLC cell lines (A549, H1299, and H1975) were selected for lentiviral transfection. The three cell lines had different characteristics: A549 is a lung adenocarcinoma cell, EGFR wild type, and resistant to gefitinib; H1299 is a lung large cell carcinoma cell, EGFR wild type, and sensitive to gefitinib; and H1975 is a lung adenocarcinoma cell, with EGFR L858R/T790M double mutations, and resistant to gefitinib but sensitive to osimertinib. This comparison was used to determine whether different characteristics of NSCLC cell lines could give consistent results. A CERS4 overexpressing murine-derived lung cancer cell line (LLC^{CERS+}) was also constructed for subsequent animal experiments. Three CERS4 stably overexpressed human-derived lung cancer cell lines and one CERS4 stably overexpressed murine-derived lung cancer cell line were constructed. The qPCR results confirmed that CERS4 was highly expressed in A549, H1299, H1975, and LLC cells after transfection (Fig. 3B and C).

Cell growth status was determined by MTT and colony formation assays to observe the change in the cell survival status after transfection. In the MTT assay (Fig. 3E), no significant difference was found in the survival status of A549, H1299, and H1975 cells after transfection. The survival curves were also observed at 24, 48, and 72 h. The two group curves were not significantly separated. In the colony formation assay, no significant difference in the number of cell clones was found when the three transfected cells were compared with the un-transfected cells (Fig. 3F and G). Thus, CERS4 overexpression did not show any

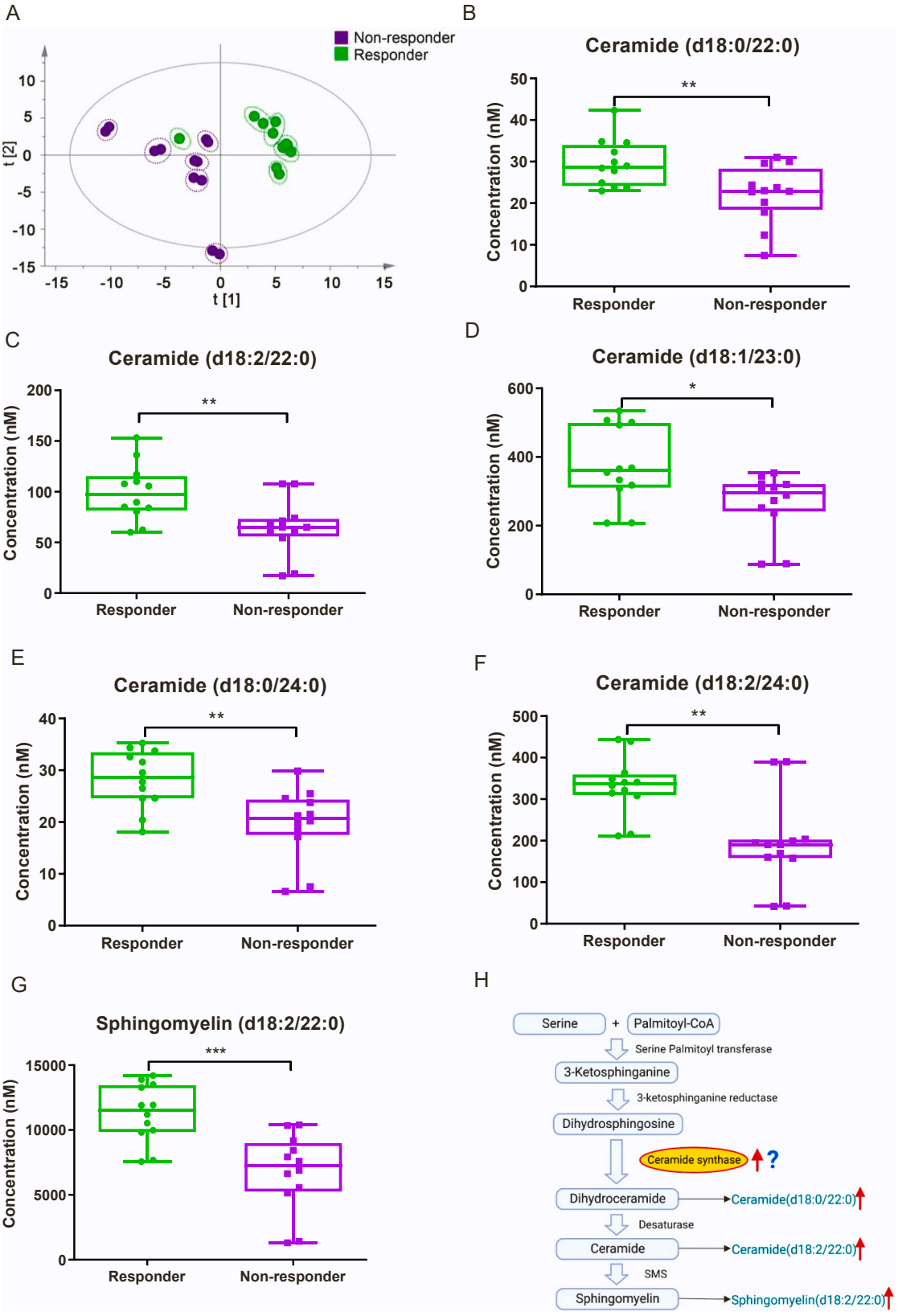

Fig. 1. Sphingolipid analysis demonstrating differences in sphingolipid metabolites between non-small cell lung cancer (NSCLC) immunotherapy responders (n = 6) and non-responders (n = 6). Each sample was analyzed in duplicate. (A) PLS-DA plot of responders' and non-responders' sphingolipid biomarkers. (B–F) Ceramide levels in serum of responders and non-responders. (G) Sphingomyelin(d18:2/22:0) levels in serum of responders and non-responders. Samples were compared using unpaired t test. (*P < 0.05, **P < 0.01, ***P < 0.001) (H) Sphingolipid metabolic pathway map.

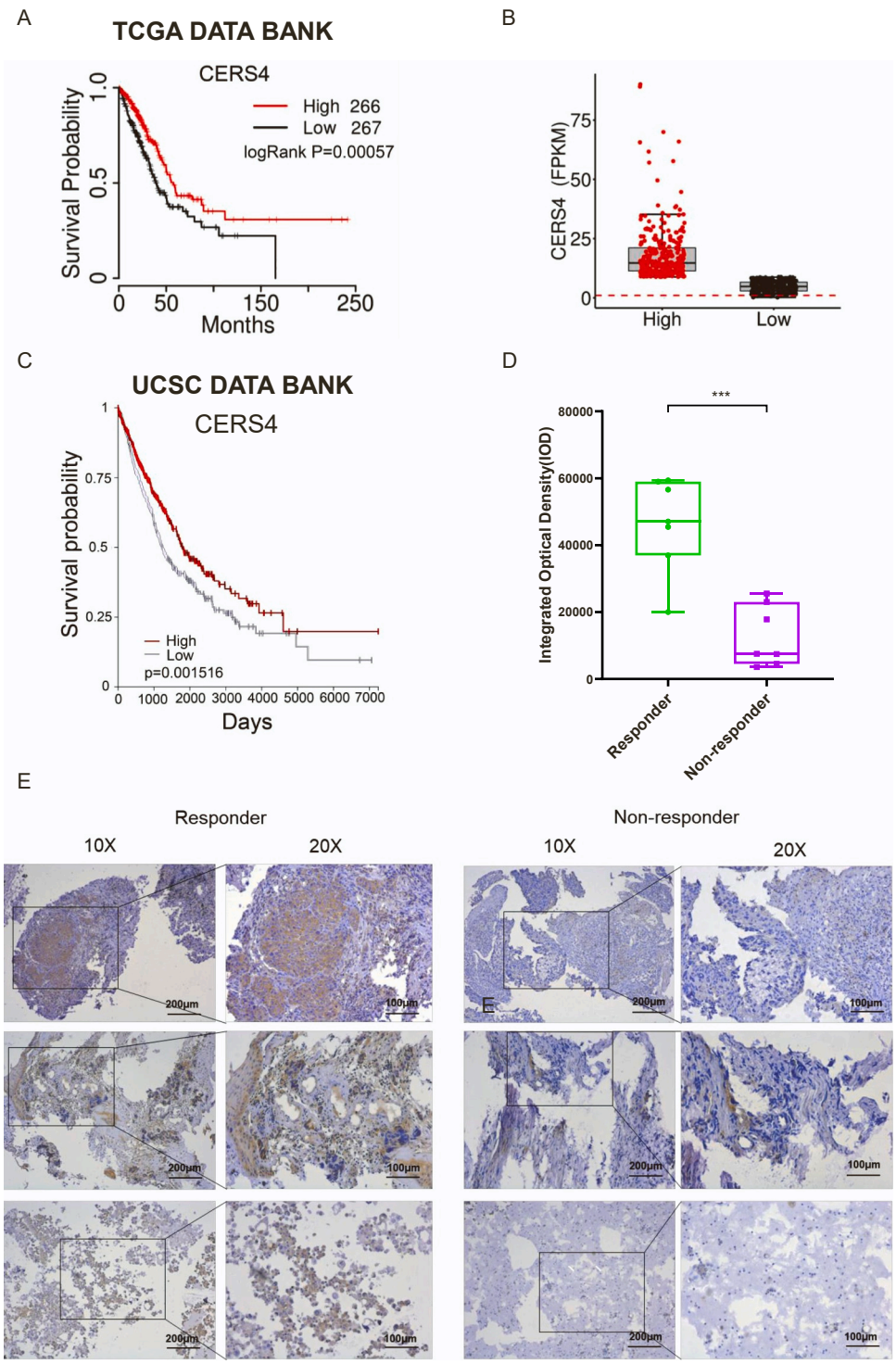

Fig. 2. Correlation of CERS4 expression with prognosis and immunotherapy response of NSCLC. (A) Survival curve of CERS4 expression in lung cancer in TCGA portal data (http://tumorsurvival.org/index.html). (B) FPKM of CERS4 in TCGA portal data, the cut off is 9, the FPKM> 9 in the high group, FPKM≤ 9 in the low group. (C) Survival curve of CERS4 expression in NSCLC in UCSC data bank. (D) Integrated optional density (IOD) value of IHC in responders and non-responders of NSCLC immunotherapy, samples were compared using unpaired t test. (*P < 0.05, **P < 0.01, ***P < 0.001) (E) CERS4 expression of tumor tissue by IHC in responders and non-responders of NSCLC immunotherapy. On the left are IHC images of three immunotherapy responders and on the right are IHC images of three immunotherapy non-responders.

significant effect on the growth viability of lung cancer cells.

3.4. Overexpression of CERS4 improves the efficacy of PD-1 mAb in mice with normal immunity

LLC and LLC^{CERS4+} cells were inoculated subcutaneously into the C57BL/6 J mice at 8–10 weeks and then treated with PD-1 mAb to further examine the role of CERS4 in modulating immunotherapy in vivo (Extended Data Fig. 4C). The results showed that the tumors in the LLC^{CERS4+} PD-1 group were significantly smaller than those in the LLC PD-1 group (Fig. 4A), and the two curves were clearly separated from day 15 onwards. Meanwhile, no significant difference in tumor size was observed in the remaining three groups (Fig. 4B). This finding indicated that no significant change in cell growth viability was observed after overexpression of CERS4 only without co-treatment with ICIs in LLC cells. After PD-1 mAb treatment was implemented, the tumors in the LLC^{CERS4+} PD-1 group were significantly smaller than those in the LLC PD-1 group, suggesting that CERS4 enhanced the efficacy of PD-1 mAb treatment. This result was consistent with the pre-predicted results. After the tumor tissues were sampled, the tumor weight in the LLC^{CERS4+} PD-1 group was significantly reduced compared with that in the LLC PD-1 group, and the difference was statistically significant (Fig. 4C).

Table 2
Clinical characteristics of 14 NSCLC patients with treatment of PD-1 mAb from Luzhou People's Hospital.

characteristics	PD-1 mAb	
	Responder	Non-responder
Age (years)	7	7
≤ 65	6	4
> 65	1	3
gender	7	7
male	4	4
female	3	3
pathology	7	7
squamous carcinoma	5	4
adenocarcinoma	2	3
TNM stage	IV	IV

Meanwhile, no significant difference was observed in the body weight of the mouse in the four groups throughout the treatment course (Extended Data Fig. 4D). In another experiment to observe animal survival, the results of survival analysis showed that the survival time of mouse in the LLC^{CERS4+} PD-1 group was significantly longer than that in the remaining three groups, whereas no significant difference was seen in the survival time of the remaining three groups (Fig. 4D). IHC detected the CERS4 expression levels in tumor tissues and found that these levels significantly increased in the two groups transfected with CERS4 (Fig. 4E). The IOD value of IHC was significantly higher in the LLC^{CERS4+} and LLC^{CERS4+} PD-1 groups (Fig. 4F). Comparison between before and after PD-1 mAb treatment revealed that this treatment may increase the CERS4 expression in tumor cells.

Overall, the overexpression of CERS4 improved the efficacy of PD-1 mAb in mice with normal immunity. The difference in in-vitro and in-vivo experiments suggested that CERS4-mediated anti-tumor response is dependent on tumor immunity.

3.5. Overexpression of CERS4 sensitizes anti-PD-1 therapy in vivo

The immune indices of mouse spleen cells and blood cells were analyzed to observe the changes in the immune environment of mice. Gating strategies were applied (Extended Data Fig. 5A). Fig. 5A represents the flow cytometric analysis of spleen cells. The proportion of $CD4^+$ T cells were significantly higher in the LLC^{CERS4+} PD-1 group than in the LLC PD-1 group, whereas the $CD8^+$ T cells showed a decreasing trend (Fig. 5B, $P < 0.05$). The $CD4^+/CD8^+$ T cell values in the LLC^{CERS4+} PD-1 group showed a significant increase compared with that in the LLC PD-1 group (Fig. 5B). Meanwhile, the percentage of Tim-3-positive cells in the LLC^{CERS4+} PD-1 group significantly decreased compared with that in the LLC PD-1 group, and the differences were statistically significant (Fig. 5B). Fig. 5C represents the flow cytometric analysis of blood cells. The gating strategies were the same as for spleen cells. Compared with the percentage of $CD4^+$ T cells in the LLC PD-1 group, that in the LLC^{CERS4+} PD-1 group showed an increasing trend, whereas the percentage of $CD8^+$ T cells showed a decreasing trend. The $CD4^+/CD8^+$ T values in the LLC^{CERS4+} PD-1 group showed a significant increase compared with those in the LLC PD-1 group (Fig. 5C). The percentage of Tim-3-positive cells in the LLC^{CERS4+} PD-1 group also significantly decreased compared with that in the LLC PD-1 group. (Fig. 5C). Overall, the overexpression of CERS4 enhanced the efficacy of PD-1 mAb by upregulating the ratio of $CD4^+/CD8^+$ T cells and downregulating Tim-3 in the immune system.

3.6. Transcriptome sequencing identified significant changes in tumor genes associated with immunity in different treatment groups

The four groups of mouse tumor tissues underwent transcriptome sequencing to identify the difference in gene transcription levels. Some genes were upregulated or downregulated in the comparison of the four groups. Compared with the LLC PD-1 group, the LLC^{CERS4+} PD-1 group had 51 upregulated and 44 downregulated genes (Fig. 6A). In the volcano plots (Fig. 6B), the left side shows the upregulated genes, and the right side shows the downregulated genes in the LLC^{CERS4+} PD-1 group compared with those in the LLC PD-1 group. The heat map (Fig. 6C) shows an obvious difference between the two groups.

The biological process (BP), cellular component (CC), and molecular function (MF) terms of the common targets from RNA sequencing were analyzed to reveal the functions of CERS4 regulation in lung cancer immunotherapy. A total of 361 GO terms were significantly enriched ($P < 0.05$), including 292 BP terms, 22 CC terms, and 47 MF terms (Extended Data Table 2). The top 25 significantly enriched terms in BP, the top 15 significantly enriched terms in CC, and the top 10 significantly enriched terms in the MF categories are displayed visually in Extended Data Fig. 6A. The results showed that the main BP terms were multicellular organism development, signal transduction, positive regulation of transcription by RNA polymerase II, and positive regulation of gene expression; the main CC terms were membrane, cytoplasm, integral component of membrane, nucleus, and plasma membrane; and the main MF terms were protein binding metal ion binding, hydrolase activity, transferase activity, and MF.

Furthermore, GO enrichment analysis was conducted on 76 common targets, and 1025 GO terms were identified ($P < 0.05$). The top 20 GO terms were selected for visual display (Extended Data Fig. 6B). The results showed that the targets were enriched mainly in the granzyme-mediated apoptotic signaling pathway, cytolysis, integrin binding, positive regulation of protein kinase B signaling, and morphogenesis of an epithelium. Most of the enriched signaling pathways were associated with immunity, indicating that CERS4 may regulate anti-PD-1 therapy by intervening in immunity-related signaling pathways.

Moreover, KEGG pathway enrichment analysis was conducted on 29 common targets, and 104 pathways were identified ($P < 0.05$). The top 20 signaling pathways were selected for visual display (Fig. 6D). The results showed that the targets were enriched mainly in the Ras signaling pathway, PI3K-Akt signaling pathway, MAPK signaling pathway, Apelin signaling pathway, and fluid shear stress and atherosclerosis. Most of the enriched signaling pathways were associated with immunity, indicating that CERS4 may regulate anti-PD-1 therapy by intervening in immunity-related signaling pathways.

3.7. Rhob, Klf2, and Rnfl82 in LLC^{CERS4+} PD-1 group are significantly downregulated compared with those in LLC PD-1 group

From the 95 differential genes identified in transcriptome sequencing, nine genes related to tumor lipid metabolism and immunotherapy were selected, including Chpt1, Cx3cl1, Cxxc4, Ptgfr, Ptn, Trmp6, Rhob, Rnf182, and Klf2 (Extended Data Fig. 7A–F and A–C). The results were verified using qPCR experiments. The qPCR results of three genes, namely, Rhob, Klf2, and Rnf182, were consistent with the transcriptomic sequencing results. Fig. 7A–C show the transcriptome sequencing results, and Fig. 7D–F show the qPCR results. All three genes were significantly lower in the LLC^{CERS4+} PD-1 group than in the LLC PD-1 group. Considering that Rhob is associated with lung cancer in more studies [33–35], this gene was chosen for the following experiment.

3.8. Rhob knockout improved the efficacy of PD-1 mAb in animal experiments

A Rhob knockout LLC cell line (LLC^{Rhob-}) was constructed to further verify whether knocking out Rhob could affect the efficacy of PD-1 mAb. Next, the LLC and LLC^{Rhob-} cells were inoculated subcutaneously into the C57BL/6 J mice at 6–8 weeks and then treated with PD-1 mAb (Extended Data Fig. 7G). The results showed that the tumors in the LLC^{Rhob-} PD-1 group were significantly smaller than those in the LLC PD-1 group (Fig. 7G), and the two curves were clearly separated from day 15

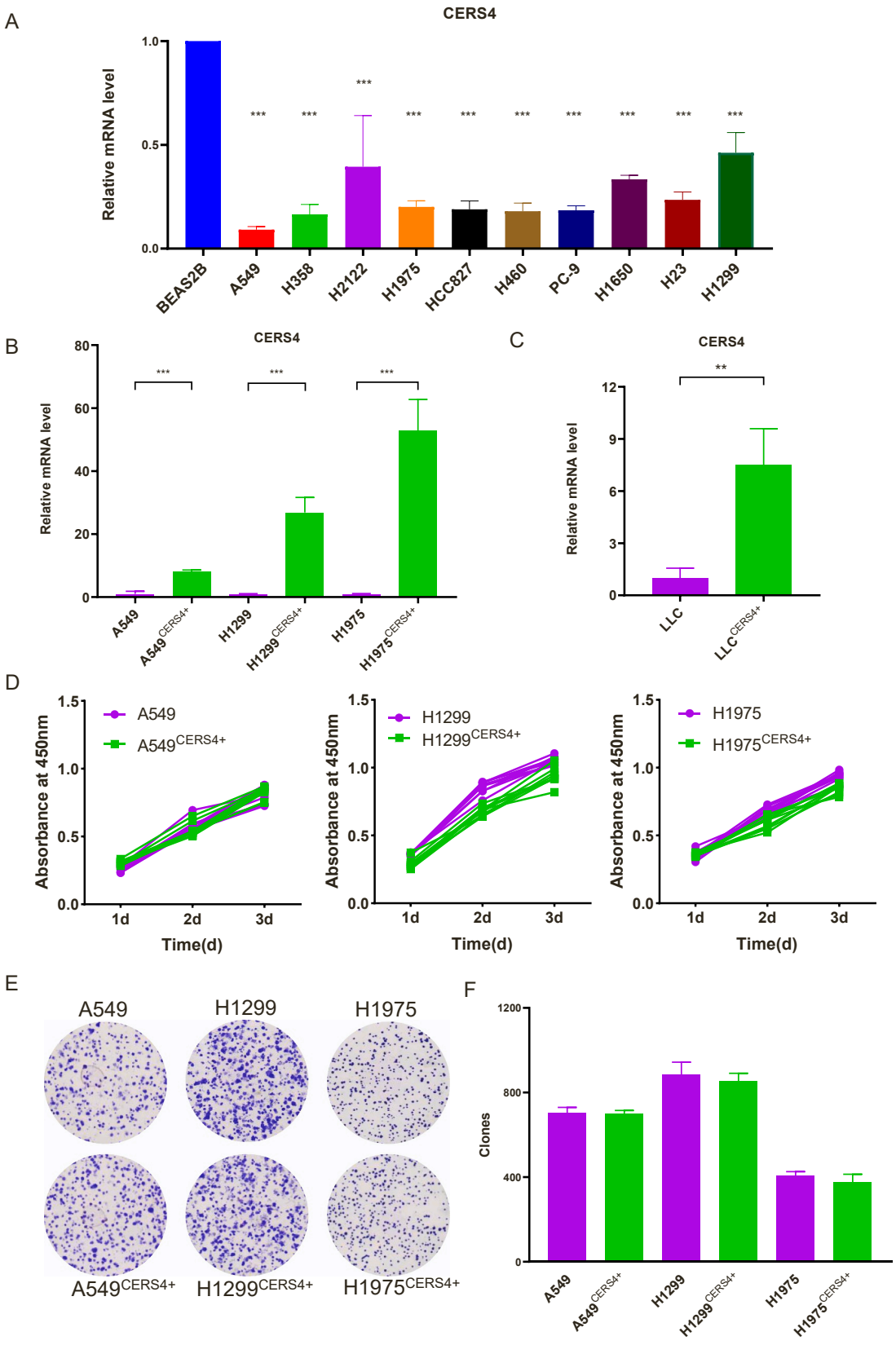

Fig. 3. Effects of CERS4 expression levels and overexpression of CERS4 in cell lines on cell growth state. (A) Quantitative CERS4 mRNA expression by qPCR in NSCLC cell lines and normal lung epithelial cell lines (BEAS2B). (B) CERS4 mRNA expression by qPCR in A549, H1299, and H1975 cell lines and after transfection with CERS4 lentiviral plasmid. (C) CERS4 mRNA expression by qPCR in LLC cell line and after transfection with CERS4 lentiviral plasmid. (D) Cell cytotoxicity levels of the cell line growth state by MTT assays. (E) Representative images of colony formation after being stained with 1% crystal violet. (F) Number of colonies counted. Data were presented as mean ± SD (n = 3). Samples were compared using unpaired t test. (*P < 0.05, **P < 0.01, ***P < 0.001).

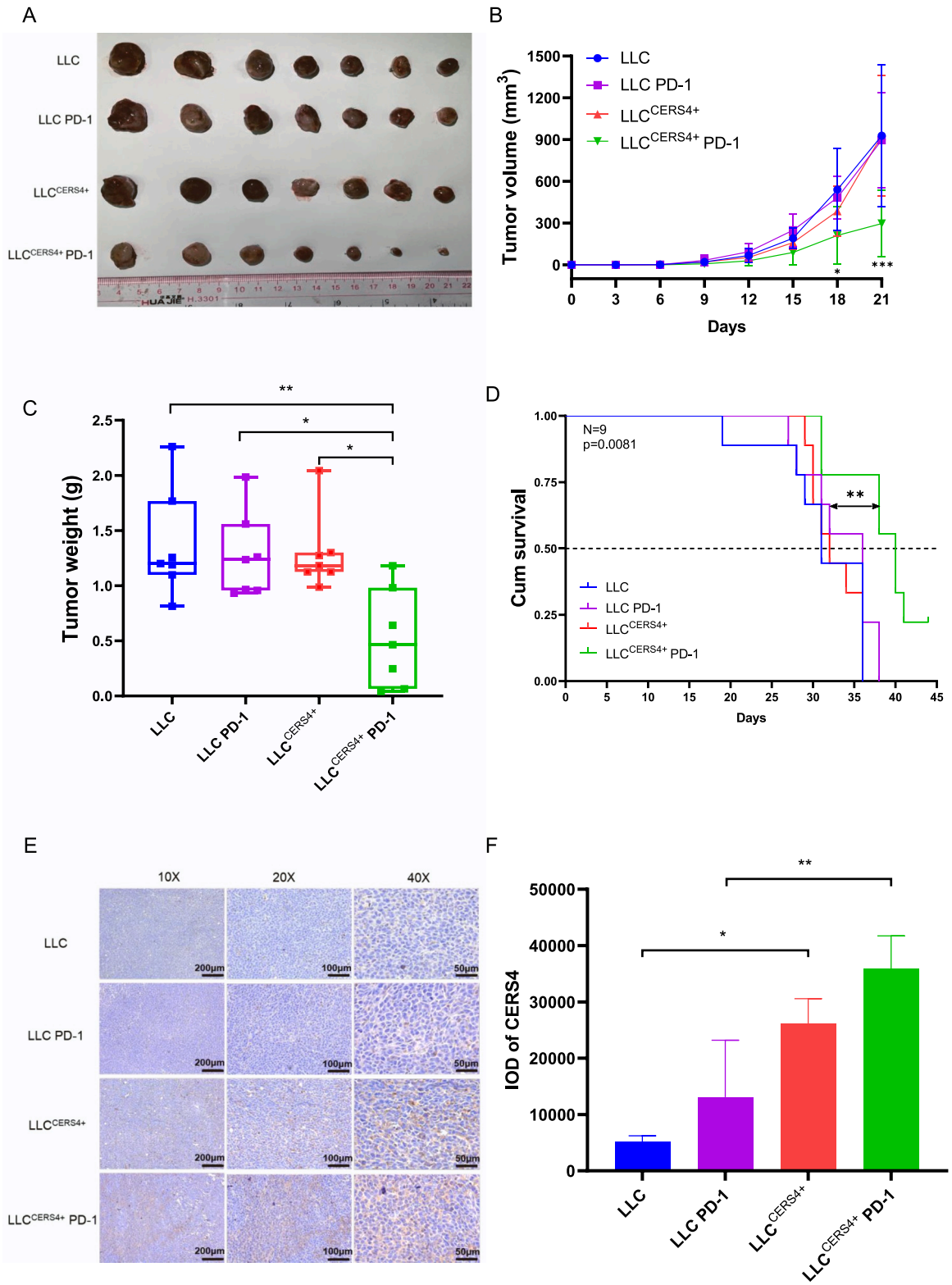

Fig. 4. Animal experiments for verification of the efficacy of immunotherapy for NSCLC after CERS4 overexpression. (A) Photographs of tumors taken after completion of animal experiments. (B) Tumor volume examined by caliper measurements from the beginning of the treatment period (when the tumor reached approximately 100 mm^3 in size), n = 7 per group. (C) Quantification of tumor weight for each group. (D) Survival time of animals for each group, n = 9 per group. (E) IHC detection of CERS4 expression in tumor tissues for each group, n = 3 per group. (F) Integrated optional density (IOD) value of IHC for each group. Samples were compared using one-way ANOVA and unpaired t test. (*P < 0.05, **P < 0.01, ***P < 0.001).

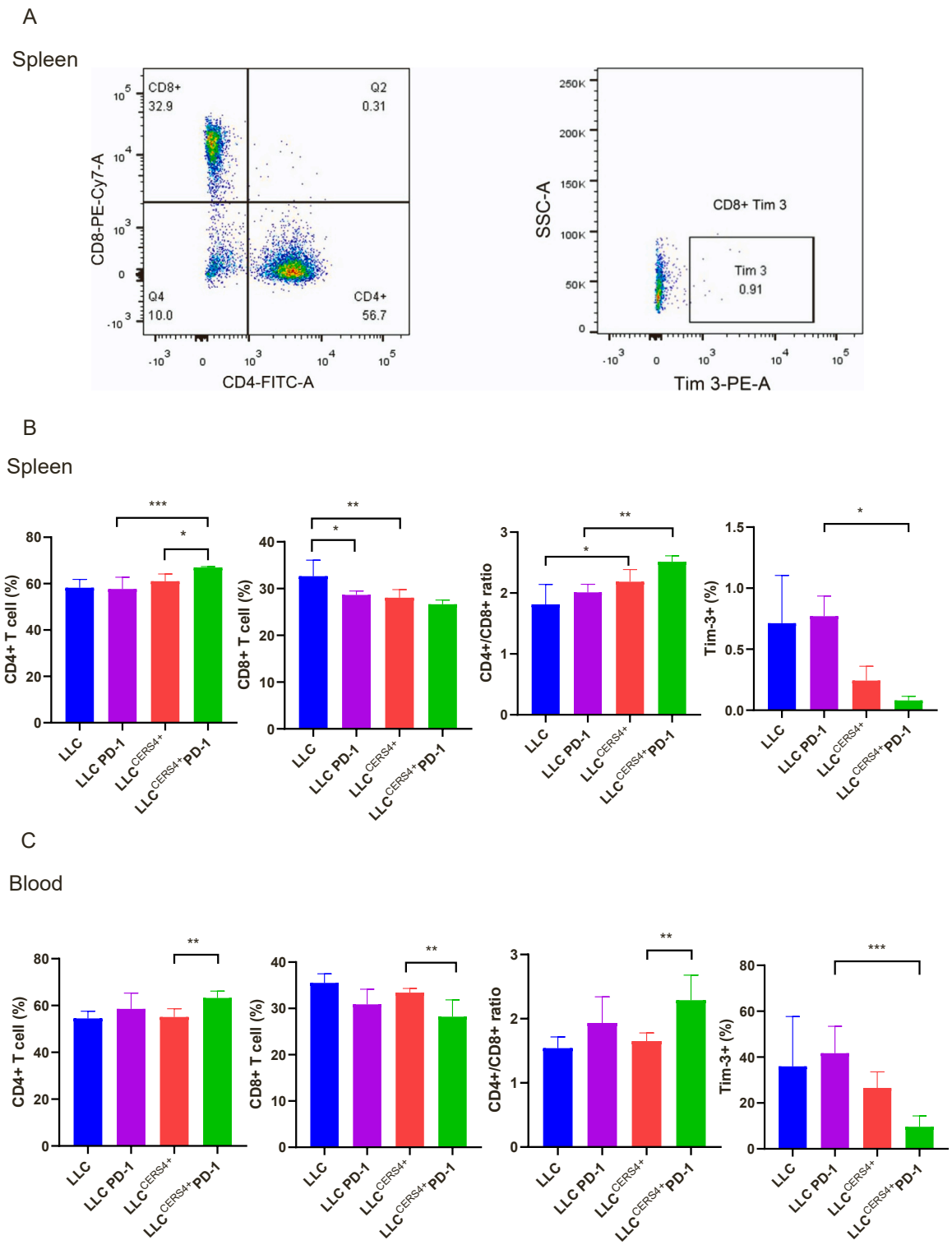

Fig. 5. Immune indices of spleen and blood cells in mice analyzed by flow cytometry. (A) Flow cytometric analysis of gating strategy diagram of spleen cells. (B) Flow cytometric detection of the percentage of $CD4^+$ T, $CD8^+$ T, and $CD8^+$ Tim-3^+ T cells in spleen cells. (C) Flow cytometric detection of the percentage of $CD4^+$ T, $CD8^+$ T, and $CD8^+$ Tim-3^+ T cells in blood cells. The results were expressed as mean ± SD. Samples were compared using one-way ANOVA. (*$P < 0.05$, **$P < 0.01$, ***$P < 0.001$).

onwards (Fig. 7H). Compared with the LLC group, the LLC^{Rhob-} group showed a decreasing trend in growth rate, but the difference was not statistically significant (Fig. 7H). After tumor tissues were sampled, the tumor weight in the LLC^{Rhob-} PD-1 group significantly decreased compared with that in the LLC PD-1 group, and the difference was statistically significant (Fig. 7I). No significant difference was found in the body weight of the mouse in the four groups throughout the treatment course (Extended Data Fig. 7H). Another animal experiment showed that the survival time of mouse in the LLC^{Rhob-} PD-1 group was significantly longer than that in the LLC PD-1 group (Fig. 7J). Therefore, knocking out Rhob improved the efficacy of PD-1 mAb in tumor-bearing mice.

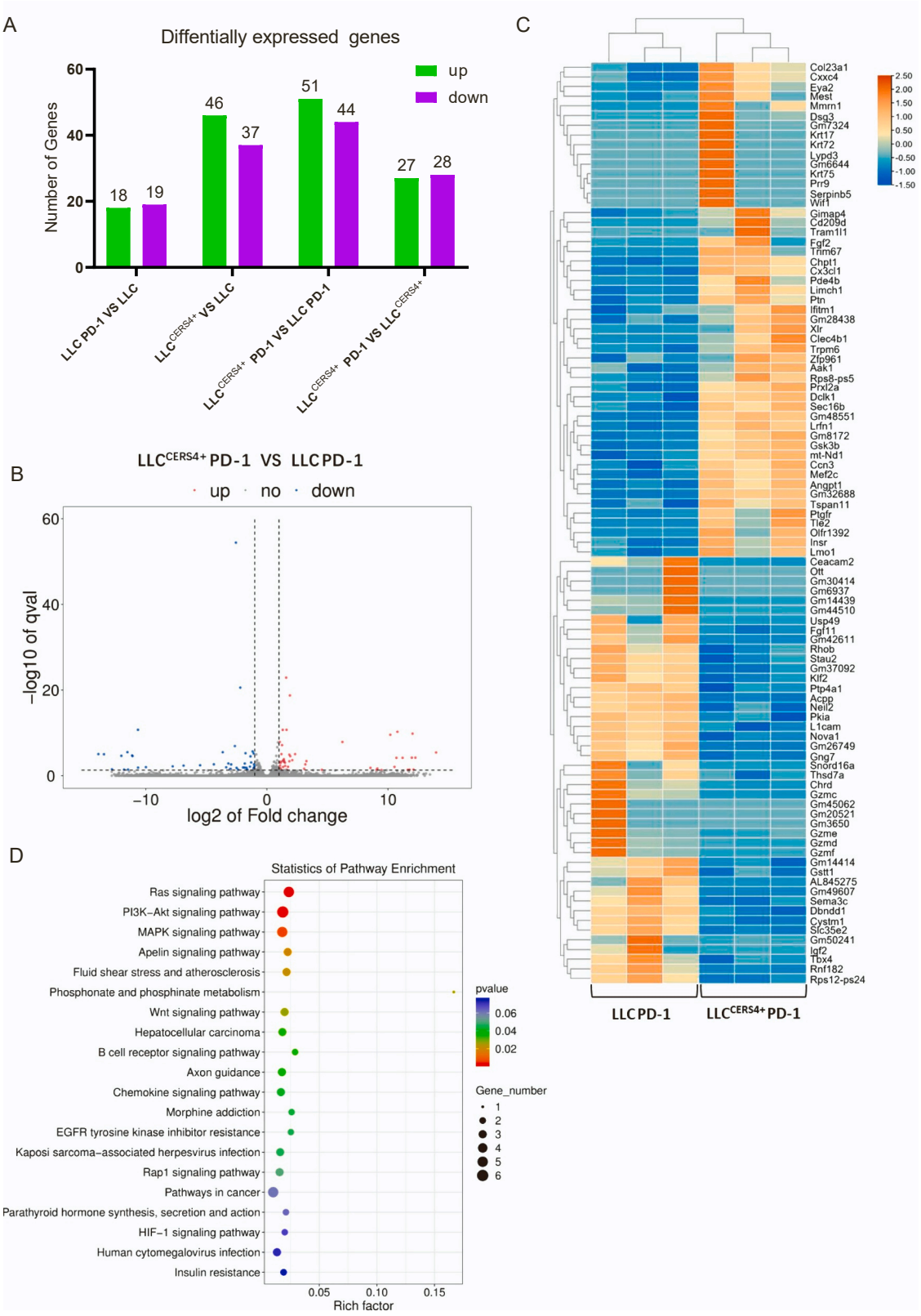

Fig. 6. Transcriptome sequencing identification of significant changes in tumor genes associated with immunity for each group. (A) Differentially expressed genes for each group. (B) Volcano plots showing upregulated genes(51) and downregulated genes(44) in the LLC^{CERS4+} PD-1 group compared with the LLC PD-1 group. (C) Heat map showing the differentially expressed genes in the LLC^{CERS4+} PD-1 group compared with the LLC PD-1 group. (D) Top 20 signaling pathways in the KEGG pathway enrichment analysis.

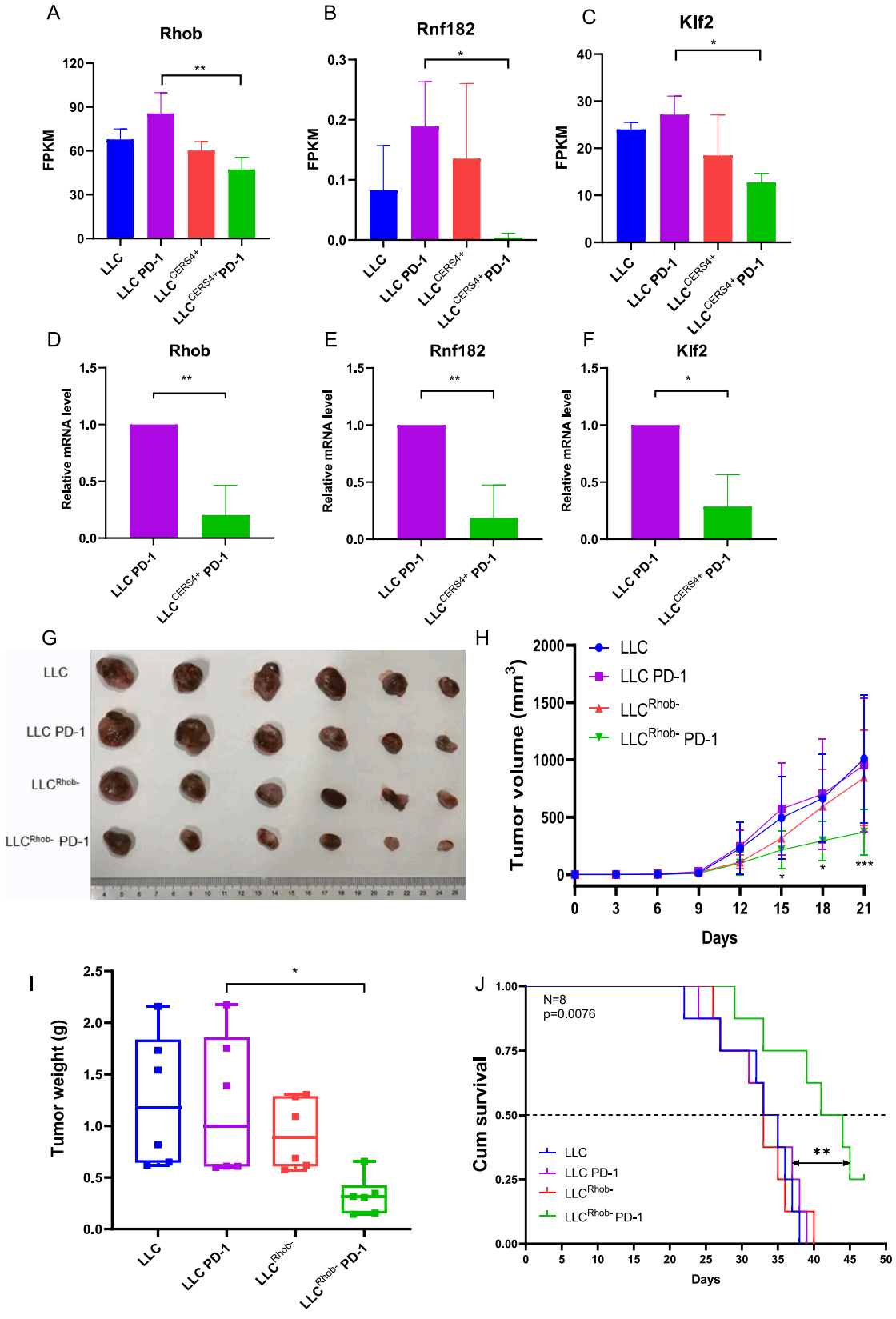

Fig. 7. Transcriptome sequencing identification of Rhob, Klf2, and Rnfl82 downregulation and verification of the efficacy of immunotherapy for NSCLC after Rhob knockout by animal experiments. (A–C) Identification of Rhob, Klf2, and Rnfl82 downregulation by transcriptome sequencing, n = 3 per group. (D–F) Verification of Rhob, Klf2, and Rnfl82 downregulation by qPCR experiment, n = 3 per group. (G) Photographs of tumors taken after completion of animal experiments. (H) Tumor volume examined by caliper measurements from the beginning of the treatment period (when the tumor reached approximately 100 mm^3 in size), n = 6 per group. (I) Quantification of tumor weight for each group, n = 6 per group. (J) Kaplan–Meier survival time of animals for each group, survival curves of four groups were compared using the Log-Rank test. n = 8 per group. Samples were compared using one-way ANOVA and unpaired t test. (*P < 0.05, **P < 0.01, ***P < 0.001).

3.9. Rhob knockout also enhanced the efficacy of PD-1 mAb by decreasing the Tim-3 level

Rhob knockout also enhanced the efficacy of PD-1 mAb. The immune profiles in spleen were analyzed by flow cytometry to observe the changes in the immune environment of mice. Compared with the LLC PD-1 group, the LLC^{Rhob-} PD-1 group demonstrated an increase in the proportion of CD4$^+$ T cells, whereas the CD8$^+$ T cells showed a decreasing trend (Fig. 8A and B). The CD4$^+$/CD8$^+$ T cell ratio in the LLC^{Rhob-} PD-1 group showed a significant increase compared with that in the LLC PD-1 group (Fig. 8C, $P < 0.05$). Meanwhile, the percentage of Tim-3-positive cells in the LLC^{Rhob-} PD-1 group was significantly reduced compared with that in the LLC PD-1 group, and the differences were statistically significant (Fig. 8D, $P < 0.01$). Overall, Rhob knockout enhanced the efficacy of PD-1 mAb by upregulating the ratio of CD4$^+$/CD8$^+$ T cells and downregulating Tim-3. This result is consistent with the previous experimental results.

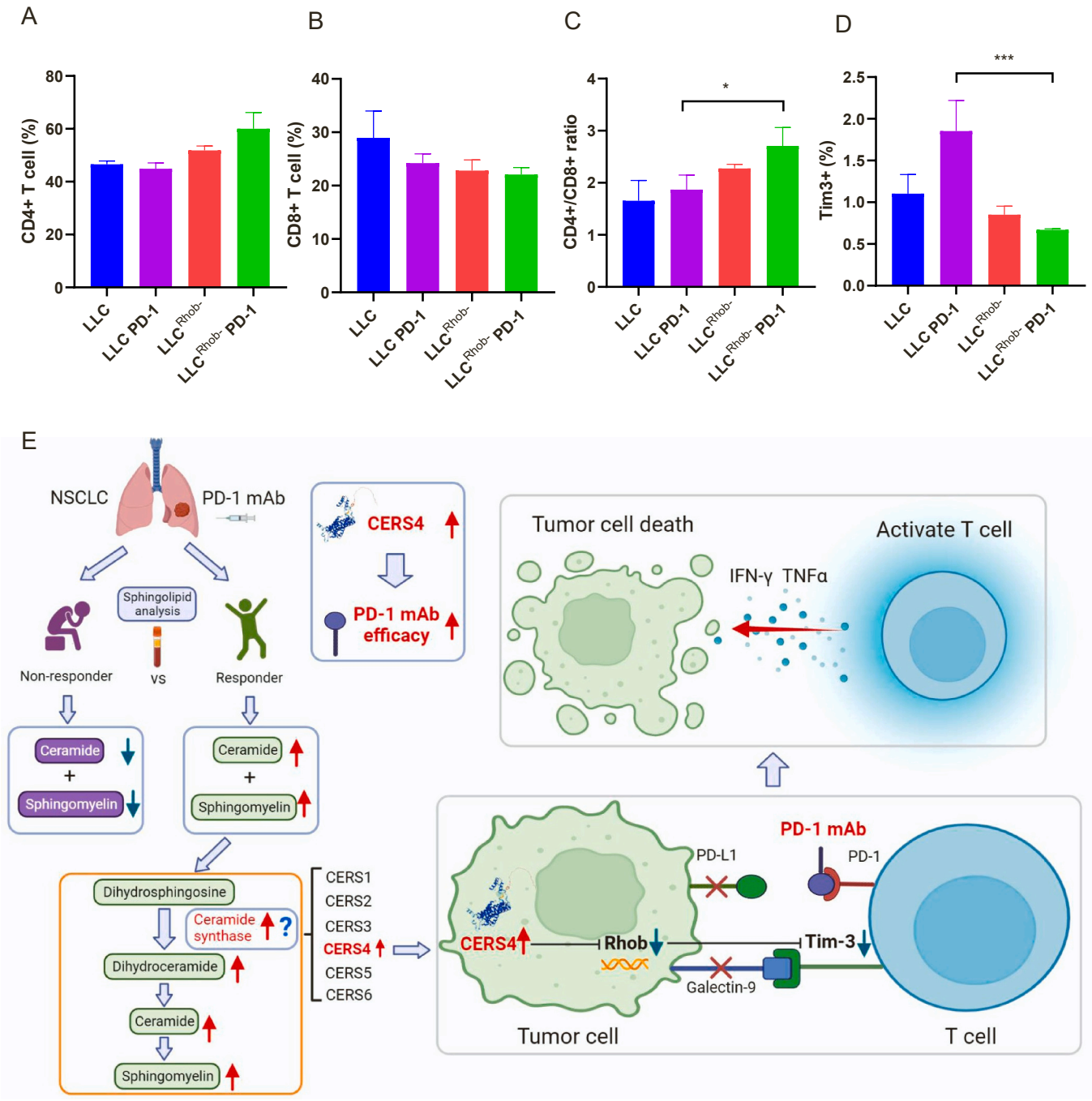

Fig. 8. Immune indices of spleen cells in mice analyzed by flow cytometry and mechanistic diagram, showing that upregulation of CERS4 enhanced the efficacy of PD-1 mAb. (A–D) Flow cytometric detection of the percentage of CD4$^+$ T, CD8$^+$ T, and CD8$^+$ Tim-3$^+$ T cells in spleen cells. The results were expressed as mean ± SD. Samples were compared using one-way ANOVA. (*$P < 0.05$, **$P < 0.01$, ***$P < 0.001$) (E) Summary of findings: the sphingolipid analysis identified that high levels of ceramides and sphingomyelin are associated with good anti-PD1 immunotherapy response. In conjunction with the sphingolipid metabolic pathway, the high expression of the metabolic enzyme ceramide synthase (CERS) was possibly responsible for this result. CERS4 was selected from six subtypes, and it was closely related to the efficacy of NSCLC immunotherapy according to clinical samples validation. Overexpression of CERS4 could improve the efficacy of anti-PD-1 by downregulating Rhob level and suppressing CD8$^+$ Tim-3$^+$ exhausted T cells.

4. Discussion

In this study, the metabolites were found to be different between PD-1 mAb therapy responders and non-responders in patients with NSCLC through the analysis of sphingolipid metabolism in clinical blood samples. CERS4 was identified as an important sphingolipid metabolic target for predicting and modulating the response of NSCLC anti-PD-1 therapy. Further studies showed that overexpression of CERS4 could improve the efficacy of anti-PD-1 by downregulating the Rhob level and suppressing $CD8^+$ $Tim\text{-}3^+$ exhausted T cells. To the authors' knowledge, this work was the first to show that the CERS4/Rhob/Tim-3 axis regulates ICIs response. Nowadays, with the high clinical demand for increased efficacy of anti-PD-1 therapy, the findings provide new predictive markers and a new target to tackle ICIs resistance in NSCLC.

The results of the article showed that CERS4 is a good prognostic gene, and patients with high CERS4 expression had better prognosis. Qian et. al. reported that high mRNA expression levels of CERS4 were associated with good prognosis in NSCLC [36], consistent with the findings in the present study. *CERS4* is an important regulatory gene of ceramide. Moreover, ceramide regulatory genes could predict the clinical prognostic risk of lung adenocarcinoma and influence the tumor immune microenvironment of lung adenocarcinoma [37]. All these data implied that CERS4 may predict lung cancer prognosis and influence tumor immune microenvironment. In addition, high CERS4 expression was found, for the first time, to have improved the efficacy of NSCLC anti-PD-1 therapy. At present, many studies on the correlation between sphingolipid metabolism and tumor immunotherapy could be found [38]. Sphingolipid metabolites are involved in the release of bioactive mediators, S1P, and ceramides, which influence the efflux and migration of lymphocytes into the tumor environment and regulate the critical pathways required for the activation of immune cells [38]. Studies have reported that C2-ceramide triggers apoptosis in melanoma cells by increasing PKCζ, pro-inflammatory cytokines, and signaling factors [39]. Another study reported that in mouse models of melanoma and breast cancer, the overexpression of wild-type nSMase2 increased anti-PD-1 efficacy [24]. These studies indicated that sphingolipid metabolites are closely related to tumor immunotherapy, which also supports the results of the present study.

In this study, mice inoculated with CERS4 overexpressing LLC cells received PD-1 mAb treatment, and sequencing of tumor tissues revealed downregulation of Rhob. This gene contains a unique c-terminal region that undergoes specific post-translational modifications that affect its localization and function [40]. Rhob is localized not only at the plasma membrane but also in the intranuclear body, multivesicular bodies, and even in the nucleus, and these unique features led to Rhob exhibiting diverse functions in the tumor microenvironment [40,41]. Luis-Ravelo et al. found that Rhob is a gene that promotes metastasis in lung adenocarcinoma, and Rhob overexpression did not alter in-situ tumor growth but led to the growth of some extra-pulmonary tumors [42]. Moreover, Rhob-depleted lung cancer cells in collagen reduced invasive capacity and increased sensitivity to paclitaxel [42]. A study by Calvayrac et al. found that low levels of Rhob expression in tumors of patients with lung cancer were correlated with good response to EGFR-TKI therapy, while high levels of Rhob corresponded to poor response [43]. Other studies have reported varying results. Loss of Rhob expression was negatively correlated with prognosis of lung cancer [44], and overexpression of Rhob could significantly inhibit tumor growth in mice [45]. In the present study, the tumor growth rate of mice inoculated with Rhob knockout LLC cells was slightly lower than that of mice inoculated with normal LLC cells, but the difference was not statistically significant. After treatment with PD-1 mAb, the tumor growth rate was significantly reduced in mice inoculated with Rhob knockout LLC cells. This result indicated that Rhob was negatively correlated with the efficacy of anti-PD-1 therapy for lung cancer. To the authors' knowledge, no study has reported this regulatory pathway, but the mechanism of Rhob regulation by CERS4 needs to be further explored.

Flow cytometric analysis found that the mice inoculated with CERS4 overexpressing or Rhob knockout LLC cells treated with PD-1 mAb had an elevated percentage of $CD4^+$ T cells, a decreased percentage of $CD8^+$ T cells, and an elevated $CD4^+/CD8^+$ ratio in the blood and spleen cells. David Y et al. reported that $CD4^+$ T cells demonstrated beneficial effects in antitumor immunotherapy, and cytotoxic $CD4^+$ T cells have direct antitumor activity [46]. Patients with cancer had higher expression levels of $CD4^+$ T cells in the responder group than in the non-responder group after the first cycle of immunotherapy [47]. Another study reported that elevated $CD8^+$ T cells are a poor prognostic factor in patients with lung adenocarcinoma, especially in patients who do not smoke [48]. Similar results were obtained in other tumors. In the peripheral blood from 80 patients with gastrointestinal cancer treated with ICIs, the baseline $CD4^+/CD8^+$ T cell ratio was lower in patients with tumor progression than in those without progression after 6 months of treatment (1.160 ± 0.652 and 1.705 ± 0.924; $P = 0.003$) [49]. Different findings have also been reported, with one study reporting that elevated PERLS ($CD8^+$ $PD\text{-}1^+/CD4^+$ $PD\text{-}1^+$) measured from blood samples prior to immunotherapy correlated with the benefit of PD-L1 blockers in NSCLC [50]. This result differs from the results of the present study, probably because the investigators tested pre-treatment samples. In addition, they did not test $CD4^+$ T and $CD8^+$ T cells but $CD4^+$ $PD\text{-}1^+$ T and $CD8^+$ $PD\text{-}1^+$ T cells. Another study showed that high $CD4^+/CD8^+$ T cell ratio was associated with poor prognosis with immunotherapy in elderly patients with lung adenocarcinoma [51], which may have a correlation with age factors. Hence, the percentage of $CD4^+$ T and $CD8^+$ T cells affect the efficacy of immunotherapy. CERS4 increases the efficacy of PD-1 mAb by downregulating Rhob and increasing the $CD4^+/CD8^+$ T cell ratio.

Downregulation of Rhob increased the efficacy of PD-1 mAb while significantly decreasing Tim-3 levels in splenocytes and blood cells. Tim-3 is an emerging target for modulating the efficacy of immunotherapy [52,53]. It marks the most terminally dysfunctional subset of $CD8^+$ TILs, and inhibition of Tim-3 enhanced the function of $CD8^+$ T cells [54]. Studies have shown that blocking Tim-3 enhanced antitumor immunotherapy efficacy in several preclinical tumor models, and Tim-3 modulated the immune cells of different cell types, thereby regulating immune responses [55]. Expression of PD-1 and Tim-3 ligands by tumor cells led to the linkage of PD-L1 to PD-1 and galectin9 to Tim-3 molecules, resulting in downregulation of T-cell function [55]. Simultaneous blockade of PD-1 and Tim-3 could have a synergistic effect, restoring T-cell effector function and tumor cell killing [55,56]. These findings are consistent with the findings of the present study, suggesting that the targeted regulation of CERS4 and Rhob genes, which enhanced the efficacy of PD-1 mAb therapy, may have resulted from lowering Tim-3 levels. High expression of CERS4 increased NSCLC anti-PD-1 therapy efficacy, decreased Rhob expression levels, and decreased Tim-3 levels in peripheral blood and splenocytes. Knockdown of Rhob similarly improved NSCLC anti-PD-1 therapy efficacy and downregulated Tim-3 expression levels, further suggesting that CERS4 improves PD-1 mAb efficacy by downregulating Rhob and Tim-3 levels. This article reported this pathway and regulatory mechanism for the first time (as shown in Fig. 8E). The results of this study provide insights into regulating NSCLC anti-PD-1 therapy efficacy.

Even though this study found that the sphingolipid metabolite target CERS4 could modulate the efficacy of NSCLC anti-PD-1 therapy and anti-PD-1 efficacy could be enhanced by regulating the CERS4/Rhob/Tim-3 axis, it still has some limitations. The CERS4/Rhob/Tim-3 axis was identified for the first time, but the underlying regulatory mechanism is still unclear. How does high CERS4 expression lead to low Rhob expression; whether it is regulated at the transcription factor level or modified at the translation level; how does low Rhob expression lead to downregulation of Tim-3 levels in immune cells, thereby modulating the efficacy of PD-1 mAb; and whether this regulatory pathway is effective in other tumor types remain unanswered. These questions need to be further explored in the future. The article demonstrated the regulatory

pathway at the cellular and mouse levels, but its validation in clinical setting needs to be confirmed by clinical studies with larger sample size.

In summary, new targets for predicting and regulating the efficacy of immunotherapy in NSCLC were identified, and the CERS4/Rhob/Tim-3 axis was found to play an essential role. This finding provides a potentially effective biomarker for the prediction of NSCLC anti-PD-1 therapy efficacy and a new idea for exploring the mechanism of anti-PD-1 therapy resistance, which is of great benefit for improving the prognosis of NSCLC anti-PD-1 therapy.

Funding

This work was funded by Dr. Neher's Biophysics Laboratory for Innovative Drug Discovery (Grant no. 001/2020/ALC), regular grants (Project no: 0003/2019/AKP, 0096/2018/A3, 0111/2020/A3, 0056/2020/AMJ & 0063/2022/A2) from Macao Science and Technology Development Fund, the National Natural Science Foundation of China (82204677), the NSFC overseas and Hong Kong and Macao Scholars Cooperative Research Fund Project (Project no: 81828013), the Science and Technology Projects in Guangzhou (SL2022A04J00459), the Technology Research Projects of State Key Laboratory of Dampness Syndrome of Chinese Medicine (no. SZ2022KF20), the Guangdong Basic and Applied Basic Research Foundation (2020B1515130005) and the 2020 Guangdong Provincial Science and Technology Innovation Strategy Special Fund (Guangdong-Hong Kong-Macau Joint Lab on Chinese Medicine and Immune Disease Research, Guangzhou University of Chinese Medicine) (No: 2020B1212030006). This work was also supported by 2020 Young Qihuang Scholar funded by National Administration of Traditional Chinese Medicine and also financially supported by the Start-up Research Grant of University of Macau (SRG2022-00020-FHS) and the Faculty of Health Sciences, University of Macau. This work is also financially supported by the FDCT Funding Scheme for Post-doctoral Researchers of Higher Education Institutions (0017/2021/APD), the 2023 State Key Laboratory of Quality Research in Chinese Medicine (UM) Internal Research Grant (IRG) (SKL-QRCM-IRG2023-001), and the FSCPO project (type 1) from Faculty of Health Sciences, University of Macau.

Declaration of Competing Interest

The authors declare no competing financial interests.

Data availability

Data will be made available on request.

Acknowledgements

Not applicable.

CRediT author statement

(I) Conception and design: ELHL, JXH, LL; (II) Administrative support: LL, ELHL; (III) Manuscript writing: All authors; (IV) Final approval of manuscript: All authors.

Statements

2. All animal experiments were approved by the Use and Care of Animals Committee at Macau University of Science and Technology. All animal experiments were performed according to committee approved protocols and institutional animal care guidelines (Registration number: A014/DICV/DIS/2019, Date: 29/8/2019).
3. The experiments complied with the WMA Statement on animal use in biomedical research and/or the and EU recommendations (Directive 2010/63/EU) for experimental design and analysis in pharmacology care and/or those of an internationally recognised body.

Appendix A. Supporting information

Supplementary data associated with this article can be found in the online version at doi:10.1016/j.phrs.2023.106850.

References

[1] H. Sung, J. Ferlay, R.L. Siegel, M. Laversanne, I. Soerjomataram, A. Jemal, F. Bray, Global cancer statistics 2020: GLOBOCAN estimates of incidence and mortality worldwide for 36 cancers in 185 countries, CA a Cancer J. Clin. 71 (3) (2021) 209–249.
[2] N. Howlader, G. Forjaz, M.J. Mooradian, R. Meza, C.Y. Kong, K.A. Cronin, A. B. Mariotto, D.R. Lowy, E.J. Feuer, The effect of advances in lung-cancer treatment on population mortality, N. Engl. J. Med 383 (7) (2020) 640–649.
[3] A.K. Ganti, A.B. Klein, I. Cotarla, B. Seal, E. Chou, Update of incidence, prevalence, survival, and initial treatment in patients with non-small cell lung cancer in the US, JAMA Oncol. 7 (12) (2021) 1824–1832.
[4] D. Planchard, S. Popat, K. Kerr, S. Novello, E.F. Smit, C. Faivre-Finn, T.S. Mok, M. Reck, P.E. Van Schil, M.D. Hellmann, S. Peters, Metastatic non-small cell lung cancer: ESMO Clinical Practice Guidelines for diagnosis, treatment and follow-up, Ann. Oncol. 29 (Suppl 4) (2018) iv192–iv237.
[5] A. Robinson, D. Vicente, A. Tafreshi, H.S. Parra, J. Mazieres, I. Cicin, B. Medgyasszay, J. Rodríguez-Cid, I. Okamoto, S. Lee, 97O First-line pembrolizumab plus chemotherapy for patients with advanced squamous NSCLC: 3-year follow-up from KEYNOTE-407, J. Thorac. Oncol. 16 (4) (2021) S748–S749.
[6] Y. Cheng, L. Zhang, J. Hu, D. Wang, C. Hu, J. Zhou, L. Wu, L. Cao, J. Liu, H. Zhang, Pembrolizumab plus chemotherapy for Chinese patients with metastatic squamous NSCLC in KEYNOTE-407, JTO Clin. Res. Rep. 2 (10) (2021), 100225.
[7] M.A. Socinski, M. Nishio, R.M. Jotte, F. Cappuzzo, F. Orlandi, D. Stroyakovskiy, N. Nogami, D. Rodríguez-Abreu, D. Moro-Sibilot, C.A. Thomas, IMpower150 final overall survival analyses for atezolizumab plus bevacizumab and chemotherapy in first-line metastatic nonsquamous NSCLC, J. Thorac. Oncol. 16 (11) (2021) 1909–1924.
[8] R.S. Herbst, G. Giaccone, F. de Marinis, N. Reinmuth, A. Vergnenegre, C.H. Barrios, M. Morise, E. Felip, Z. Andric, S. Geater, M. Özgüroğlu, W. Zou, A. Sandler, I. Enquist, K. Komatsubara, Y. Deng, H. Kuriki, X. Wen, M. McCleland, S. Mocci, J. Jassem, D.R. Spigel, Atezolizumab for first-line treatment of PD-L1-selected patients with NSCLC, N. Engl. J. Med 383 (14) (2020) 1328–1339.
[9] D.P. Carbone, M. Reck, L. Paz-Ares, B. Creelan, L. Horn, M. Steins, E. Felip, M. M. van den Heuvel, T.E. Ciuleanu, F. Badin, N. Ready, T.J.N. Hiltermann, S. Nair, R. Juergens, S. Peters, E. Minenza, J.M. Wrangle, D. Rodriguez-Abreu, H. Borghaei, G.R. Blumenschein Jr., L.C. Villaruz, L. Havel, J. Krejci, J. Corral Jaime, H. Chang, W.J. Geese, P. Bhagavatheeswaran, A.C. Chen, M.A. Socinski, First-line nivolumab in stage IV or recurrent non-small-cell lung cancer, N. Engl. J. Med. 376 (25) (2017) 2415–2426.
[10] E.B. Garon, M.D. Hellmann, N.A. Rizvi, E. Carcereny, N.B. Leighl, M.-J. Ahn, J. P. Eder, A.S. Balmanoukian, C. Aggarwal, L. Horn, A. Patnaik, M. Gubens, S. S. Ramalingam, E. Felip, J.W. Goldman, C. Scalzo, E. Jensen, D.A. Kush, R. Hui, Five-Year Overall survival for patients with advanced non-small-cell lung cancer treated with pembrolizumab: results from the phase I KEYNOTE-001 study, J. Clin. Oncol. 37 (28) (2019) 2518–2527.
[11] M.D. Hellmann, T.E. Ciuleanu, A. Pluzanski, J.S. Lee, G.A. Otterson, C. Audigier-Valette, E. Minenza, H. Linardou, S. Burgers, P. Salman, H. Borghaei, S. S. Ramalingam, J. Brahmer, M. Reck, K.J. O'Byrne, W.J. Geese, G. Green, H. Chang, J. Szustakowski, P. Bhagavatheeswaran, D. Healey, Y. Fu, F. Nathan, L. Paz-Ares, Nivolumab plus Ipilimumab in lung cancer with a high tumor mutational burden, N. Engl. J. Med. 378 (22) (2018) 2093–2104.
[12] A. Marabelle, M. Fakih, J. Lopez, M. Shah, R. Shapira-Frommer, K. Nakagawa, H. C. Chung, H.L. Kindler, J.A. Lopez-Martin, W.H. Miller Jr., A. Italiano, S. Kao, S. A. Piha-Paul, J.P. Delord, R.R. McWilliams, D.A. Fabrizio, D. Aurora-Garg, L. Xu, F. Jin, K. Norwood, Y.J. Bang, Association of tumour mutational burden with outcomes in patients with advanced solid tumours treated with pembrolizumab: prospective biomarker analysis of the multicohort, open-label, phase 2 KEYNOTE-158 study, Lancet Oncol. 21 (10) (2020) 1353–1365.
[13] M.F. Sanmamed, L. Chen, A paradigm shift in cancer immunotherapy: from enhancement to normalization, Cell 175 (2) (2018) 313–326.
[14] B. Rousseau, M.B. Foote, S.B. Maron, B.H. Diplas, S. Lu, G. Argilés, A. Cercek, L. A. Diaz Jr., The spectrum of benefit from checkpoint blockade in hypermutated tumors, N. Engl. J. Med. 384 (12) (2021) 1168–1170.
[15] R.J. Hause, C.C. Pritchard, J. Shendure, S.J. Salipante, Classification and characterization of microsatellite instability across 18 cancer types, Nat. Med. 22 (11) (2016) 1342–1350.
[16] F. Bie, H. Tian, N. Sun, R. Zang, M. Zhang, P. Song, L. Liu, Y. Peng, G. Bai, B. Zhou, S. Gao, Research progress of Anti-PD-1/PD-L1 immunotherapy related mechanisms and predictive biomarkers in NSCLC, Front. Oncol. 12 (2022), 769124.
[17] M. Wang, R.S. Herbst, C. Boshoff, Toward personalized treatment approaches for non-small-cell lung cancer, Nat. Med. 27 (8) (2021) 1345–1356.
[18] R.Z. Li, X.R. Wang, J. Wang, C. Xie, X.X. Wang, H.D. Pan, W.Y. Meng, T.L. Liang, J. X. Li, P.Y. Yan, Q.B. Wu, L. Liu, X.J. Yao, E.L. Leung, The key role of sphingolipid

metabolism in cancer: New therapeutic targets, diagnostic and prognostic values, and anti-tumor immunotherapy resistance, Front Oncol. 12 (2022), 941643.
[19] B. Ogretmen, Sphingolipid metabolism in cancer signalling and therapy, Nat. Rev. Cancer 18 (1) (2018) 33–50.
[20] Y. Wang, M.S. Bhave, H. Yagita, S.L. Cardell, Natural killer T-cell agonist α-galactosylceramide and PD-1 blockade synergize to reduce tumor development in a preclinical model of colon cancer, Front Immunol. 11 (2020), 581301.
[21] L. Zhang, A. Donda, Redirecting iNKT cell antitumor immunity with α-GalCer/CD1d-scFv fusion proteins, Methods Mol. Biol. 2388 (2021) 175–180.
[22] P. Chakraborty, S.G. Vaena, K. Thyagarajan, S. Chatterjee, A. Al-Khami, S. P. Selvam, H. Nguyen, I. Kang, M.W. Wyatt, U. Baliga, Pro-survival lipid sphingosine-1-phosphate metabolically programs T cells to limit anti-tumor activity, Cell Rep. 28 (7) (2019) 1879–1893, e7.
[23] C. Imbert, A. Montfort, M. Fraisse, E. Marcheteau, J. Gilhodes, E. Martin, F. Bertrand, M. Marcellin, O. Burlet-Schiltz, A.Gd Peredo, V. Garcia, S. Carpentier, S. Tartare-Deckert, P. Brousset, P. Rochaix, F. Puisset, T. Filleron, N. Meyer, L. Lamant, T. Levade, B. Ségui, N. Andrieu-Abadie, C. Colacios, Resistance of melanoma to immune checkpoint inhibitors is overcome by targeting the sphingosine kinase-1, Nat. Commun. 11 (1) (2020) 437.
[24] A. Montfort, F. Bertrand, J. Rochotte, J. Gilhodes, T. Filleron, J. Milhès, C. Dufau, C. Imbert, J. Riond, M. Tosolini, C.J. Clarke, F. Dufour, A.A. Constantinescu, N. F. Junior, V. Garcia, M. Record, P. Cordelier, P. Brousset, P. Rochaix, S. Silvente-Poirot, N. Therville, N. Andrieu-Abadie, T. Levade, Y.A. Hannun, H. Benoist, N. Meyer, O. Micheau, C. Colacios, B. Ségui, Neutral sphingomyelinase 2 heightens anti-melanoma immune responses and anti-PD-1 therapy efficacy, Cancer Immunol. Res 9 (5) (2021) 568–582.
[25] I.Y. Cheung, N.V. Cheung, S. Modak, A. Mauguen, Y. Feng, E. Basu, S.S. Roberts, G. Ragupathi, B.H. Kushner, Survival impact of anti-GD2 antibody response in a phase II ganglioside vaccine trial among patients with high-risk neuroblastoma with prior disease progression, J. Clin. Oncol. Off. J. Am. Soc. Clin. Oncol. 39 (3) (2021) 215–226.
[26] T. Toyoda, T. Kamata, K. Tanaka, F. Ihara, M. Takami, H. Suzuki, T. Nakajima, T. Ikeuchi, Y. Kawasaki, H. Hanaoka, T. Nakayama, I. Yoshino, S. Motohashi, Phase II study of α-galactosylceramide-pulsed antigen-presenting cells in patients with advanced or recurrent non-small cell lung cancer, J. Immunother. Cancer 8 (1) (2020), e000316.
[27] Y. Su, J. Huang, S. Wang, J.M. Unger, J. Arias-Fuenzalida, Y. Shi, J. Li, Y. Gao, W. Shi, X. Wang, R. Peng, F. Xu, X. An, C. Xue, W. Xia, R. Hong, Y. Zhong, Y. Lin, H. Huang, A. Zhang, L. Zhang, L. Cai, J. Zhang, Z. Yuan, The effects of ganglioside-monosialic acid in taxane-induced peripheral neurotoxicity in patients with breast cancer: a randomized trial, J. Natl. Cancer Inst. 112 (1) (2020) 55–62.
[28] J.R. Wang, H. Zhang, L.F. Yau, J.N. Mi, S. Lee, K.C. Lee, P. Hu, L. Liu, Z.H. Jiang, Improved sphingolipidomic approach based on ultra-high performance liquid chromatography and multiple mass spectrometries with application to cellular neurotoxicity, Anal. Chem. 86 (12) (2014) 5688–5696.
[29] R. Tidhar, I.D. Zelnik, G. Volpert, S. Ben-Dor, S. Kelly, A.H. Merrill Jr., A. H. Futerman, Eleven residues determine the acyl chain specificity of ceramide synthases, J. Biol. Chem. 293 (25) (2018) 9912–9921.
[30] T. Sassa, T. Hirayama, A. Kihara, Enzyme activities of the ceramide synthases CERS2-6 are regulated by phosphorylation in the C-terminal region, J. Biol. Chem. 291 (14) (2016) 7477–7487.
[31] C. Robert, J. Schachter, G.V. Long, A. Arance, J.J. Grob, L. Mortier, A. Daud, M. S. Carlino, C. McNeil, M. Lotem, J. Larkin, P. Lorigan, B. Neyns, C.U. Blank, O. Hamid, C. Mateus, R. Shapira-Frommer, M. Kosh, H. Zhou, N. Ibrahim, S. Ebbinghaus, A. Ribas, Pembrolizumab versus Ipilimumab in Advanced Melanoma, N. Engl. J. Med 372 (26) (2015) 2521–2532.
[32] A. Ribas, I. Puzanov, R. Dummer, D. Schadendorf, O. Hamid, C. Robert, F.S. Hodi, J. Schachter, A.C. Pavlick, K.D. Lewis, L.D. Cranmer, C.U. Blank, S.J. O'Day, P. A. Ascierto, A.K. Salama, K.A. Margolin, C. Loquai, T.K. Eigentler, T.C. Gangadhar, M.S. Carlino, S.S. Agarwala, S.J. Moschos, J.A. Sosman, S.M. Goldinger, R. Shapira-Frommer, R. Gonzalez, J.M. Kirkwood, J.D. Wolchok, A. Eggermont, X.N. Li, W. Zhou, A.M. Zernhelt, J. Lis, S. Ebbinghaus, S.P. Kang, A. Daud, Pembrolizumab versus investigator-choice chemotherapy for ipilimumab-refractory melanoma (KEYNOTE-002): a randomised, controlled, phase 2 trial, Lancet Oncol. 16 (8) (2015) 908–918.
[33] O. Calvayrac, A. Pradines, G. Favre, RHOB expression controls the activity of serine/threonine protein phosphatase PP2A to modulate mesenchymal phenotype and invasion in non-small cell lung cancers, Small GTPases 9 (4) (2018) 339–344.
[34] C. Laplagne, S. Meddour, S. Figarol, M. Michelas, O. Calvayrac, G. Favre, C. Laurent, J.J. Fournié, S. Cabantous, M. Poupot, V. γ9Vδ2, T. Cells, Activation through phosphoantigens can be impaired by a RHOB rerouting in lung cancer, Front Immunol. 11 (2020) 1396.
[35] O. Calvayrac, A. Nowosad, S. Cabantous, L.P. Lin, S. Figarol, P. Jeannot, M. P. Serres, C. Callot, R.T. Perchey, J. Creff, E. Taranchon-Clermont, I. Rouquette, G. Favre, A. Pradines, S. Manenti, J. Mazieres, H. Lee, A. Besson, Cytoplasmic p27 (Kip1) promotes tumorigenesis via suppression of RhoB activity, J. Pathol. 247 (1) (2019) 60–71.
[36] H. Qian, J. Deng, C. Lu, G. Hou, H. Zhang, M. Zhang, Z. Fang, X.-D. Lv, Ceramide synthases: insights into the expression and prognosis of lung cancer, Exp. Lung Res 47 (1) (2021) 37–53.
[37] Y. Zhang, J. Chen, Y. Zhao, L. Weng, Y. Xu, Ceramide pathway regulators predict clinical prognostic risk and affect the tumor immune microenvironment in lung adenocarcinoma, Front Oncol. 10 (2020), 562574.
[38] P. Giussani, A. Prinetti, C. Tringali, The role of sphingolipids in cancer immunotherapy, Int J. Mol. Sci. 22 (12) (2021) 6492.
[39] S. Ghosh, S.K. Juin, P. Nandi, S.B. Majumdar, A. Bose, R. Baral, P.C. Sil, S. Majumdar, PKCζ mediated anti-proliferative effect of C2 ceramide on neutralization of the tumor microenvironment and melanoma regression, Cancer Immunol. Immunother. 69 (4) (2020) 611–627.
[40] F.M. Vega, A.J. Ridley, The RhoB small GTPase in physiology and disease, Small GTPases 9 (5) (2018) 384–393.
[41] J.A. Ju, D.M. Gilkes, RhoB: team oncogene or team tumor suppressor? Genes 9 (2) (2018) 67.
[42] D. Luis-Ravelo, I. Antón, C. Zandueta, K. Valencia, M.J. Pajares, J. Agorreta, L. Montuenga, S. Vicent, Wistuba II, J. De Las Rivas, F. Lecanda, RHOB influences lung adenocarcinoma metastasis and resistance in a host-sensitive manner, Mol. Oncol. 8 (2) (2014) 196–206.
[43] O. Calvayrac, J. Mazières, S. Figarol, C. Marty-Detraves, I. Raymond-Letron, E. Bousquet, M. Farella, E. Clermont-Taranchon, J. Milia, I. Rouquette, N. Guibert, A. Lusque, J. Cadranel, N. Mathiot, A. Savina, A. Pradines, G. Favre, The RAS-related GTPase RHOB confers resistance to EGFR-tyrosine kinase inhibitors in non-small-cell lung cancer via an AKT-dependent mechanism, EMBO Mol. Med 9 (2) (2017) 238–250.
[44] N. Sato, T. Fukui, T. Taniguchi, T. Yokoyama, M. Kondo, T. Nagasaka, Y. Goto, W. Gao, Y. Ueda, K. Yokoi, J.D. Minna, H. Osada, Y. Kondo, Y. Sekido, RhoB is frequently downregulated in non-small-cell lung cancer and resides in the 2p24 homozygous deletion region of a lung cancer cell line, Int J. Cancer 120 (3) (2007) 543–551.
[45] J. Mazieres, T. Antonia, G. Daste, C. Muro-Cacho, D. Berchery, V. Tillement, A. Pradines, S. Sebti, G. Favre, Loss of RhoB expression in human lung cancer progression, Clin. Cancer Res 10 (8) (2004) 2742–2750.
[46] D.Y. Oh, L. Fong, Cytotoxic CD4(+) T cells in cancer: Expanding the immune effector toolbox, Immunity 54 (12) (2021) 2701–2711.
[47] B. Xenia Elena, L. Nicoleta Gales, A. Florina Zgura, L. Iliescu, R. Maricela Anghel, B. Haineala, Assessment of immune status in dynamics for patients with cancer undergoing immunotherapy, J. Oncol. 2021 (2021), 6698969.
[48] T. Kinoshita, C. Kudo-Saito, R. Muramatsu, T. Fujita, M. Saito, H. Nagumo, T. Sakurai, S. Noji, E. Takahata, T. Yaguchi, N. Tsukamoto, Y. Hayashi, K. Kaseda, I. Kamiyama, T. Ohtsuka, K. Tomizawa, M. Shimoji, T. Mitsudomi, H. Asamura, Y. Kawakami, Determination of poor prognostic immune features of tumour microenvironment in non-smoking patients with lung adenocarcinoma, Eur. J. Cancer 86 (2017) 15–27.
[49] C. Liu, Y. Wang, S. Li, X. Jiao, J. Zou, Z. Wang, C. Qi, X. Zhang, J. Li, Z. Lu, L. Shen, Early change in peripheral CD4(+) T cells associated with clinical outcomes of immunotherapy in gastrointestinal cancer, Immunotherapy 13 (1) (2021) 55–66.
[50] B. Duchemann, M. Naigeon, E. Auclin, R. Ferrara, L. Cassard, J.M. Jouniaux, L. Boselli, J. Grivel, A. Desnoyer, F.X. Danlos, L. Mezquita, C. Caramella, A. Marabelle, B. Besse, N. Chaput, CD8(+)PD-1(+) to CD4(+)PD-1(+) ratio (PERLS) is associated with prognosis of patients with advanced NSCLC treated with PD-(L)1 blockers, J. Immunother. Cancer 10 (2) (2022).
[51] M. Ilié, M. Beaulande, S. Ben Hadj, E. Chamorey, R. Schiappa, E. Long-Mira, S. Lassalle, C. Butori, C. Cohen, S. Leroy, O. Guérin, J. Mouroux, C.H. Marquette, J. F. Pomerol, G. Erb, V. Hofman, P. Hofman, Chromogenic multiplex immunohistochemistry reveals modulation of the immune microenvironment associated with survival in elderly patients with lung adenocarcinoma, Cancers 10 (9) (2018) 326.
[52] L. Kraehenbuehl, C.H. Weng, S. Eghbali, J.D. Wolchok, T. Merghoub, Enhancing immunotherapy in cancer by targeting emerging immunomodulatory pathways, Nat. Rev. Clin. Oncol. 19 (1) (2022) 37–50.
[53] N. Acharya, C. Sabatos-Peyton, A.C. Anderson, Tim-3 finds its place in the cancer immunotherapy landscape, J. Immunother. Cancer 8 (1) (2020), e000911.
[54] H.T. Jin, A.C. Anderson, W.G. Tan, E.E. West, S.J. Ha, K. Araki, G.J. Freeman, V. K. Kuchroo, R. Ahmed, Cooperation of Tim-3 and PD-1 in CD8 T-cell exhaustion during chronic viral infection, Proc. Natl. Acad. Sci. USA 107 (33) (2010) 14733–14738.
[55] M. Das, C. Zhu, V.K. Kuchroo, Tim-3 and its role in regulating anti-tumor immunity, Immunol. Rev. 276 (1) (2017) 97–111.
[56] G. Curigliano, H. Gelderblom, N. Mach, T. Doi, D. Tai, P.M. Forde, J. Sarantopoulos, P.L. Bedard, C.C. Lin, F.S. Hodi, S. Wilgenhof, A. Santoro, C.A. Sabatos-Peyton, T.A. Longmire, A. Xyrafas, H. Sun, S. Gutzwiller, L. Manenti, A. Naing, Phase I/Ib Clinical Trial of Sabatolimab, an Anti-TIM-3 Antibody, Alone and in Combination with Spartalizumab, an Anti-PD-1 Antibody, in Advanced Solid Tumors, Clinical cancer research: an official journal of the American Association for Cancer Research 27(13) (2021) 3620–3629.